

Synthesis and Characterization of $\text{Fe}_3\text{O}_4@\text{TiO}_2$ for Drug Delivery Applications



By

Anum Rabab

(Registration No: 00000329200)

Department of Materials Engineering

School of Chemical and Materials Engineering

National University of Sciences & Technology (NUST)

Islamabad, Pakistan

(2024)

Synthesis and Characterization of $\text{Fe}_3\text{O}_4@ \text{TiO}_2$ for Drug Delivery Applications



By

Anum Rabab

(Registration No: 00000329200)

A thesis submitted to the National University of Sciences and Technology, Islamabad,

in partial fulfillment of the requirements for the degree of

Master of Science in

Materials Engineering

Supervisor: Dr. Iftikhar Hussain Gul

School of Chemical and Materials Engineering

National University of Sciences & Technology (NUST)

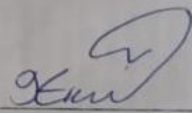
Islamabad, Pakistan

(2024)



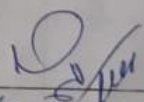
THESIS ACCEPTANCE CERTIFICATE

Certified that final copy of MS thesis written by Ms **Anum Rabab** (Registration No 00000329200), of School of Chemical & Materials Engineering (SCME) has been vetted by undersigned, found complete in all respects as per NUST Statues/Regulations, is free of plagiarism, errors, and mistakes and is accepted as partial fulfillment for award of MS degree. It is further certified that necessary amendments as pointed out by GEC members of the scholar have also been incorporated in the said thesis.

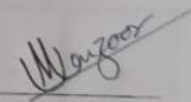
Signature: _____ 

Name of Supervisor: **Dr Iftikhar Hussian Gul**

Date: 8/10/2024

Signature (HOD): _____ 

Date: 10/10/24

Signature (Dean/Principal): _____ 

Date: 10/10/24



National University of Sciences & Technology (NUST)

FORM TH-4

MASTER'S THESIS WORK

We hereby recommend that the dissertation prepared under our supervision by

Regn No & Name: 00000329200 Anum Rabab

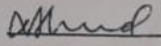
Title: Synthesis & Characterization of $\text{Fe}_3\text{O}_4@ \text{TIO}_2$ for Drug Delivery Applications

Presented on: 28 Aug 2024 at: 1500 hrs in SCME Seminar Hall

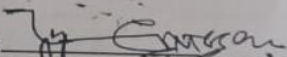
Be accepted in partial fulfillment of the requirements for the award of Masters of Science degree in Materials & Surface Engineering.

Guidance & Examination Committee Members

Name: Dr Nasir M. Ahmed

Signature: 

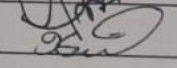
Name: Dr Zakir Hussain

Signature: 

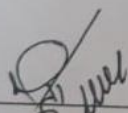
Name: Dr Usman Liaqat (Co-Supervisor)

Signature: 

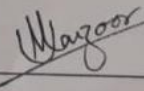
Supervisor's Name: Dr Iftikhar Hussain Gul

Signature: 

Dated: 28/8/2024


Head of Department

Date 05-09-24


Dean/Principal

Date 5/9/24

School of Chemical & Materials Engineering (SCME)

AUTHOR'S DECLARATION

I Anum Rabab hereby state that my MS thesis titled "Synthesis and characterization of Fe₃O₄@ TiO₂ for drug delivery applications" is my own work and has not been submitted previously by me for taking any degree from National University of Sciences and Technology, Islamabad or anywhere else in the country/ world.

At any time if my statement is found to be incorrect even after I graduate, the university has the right to withdraw my MS degree.

Name of Student: Anum Rabab

Date: 01/ 10/ 2024

PLAGIARISM UNDERTAKING

I solemnly declare that research work presented in the thesis titled “Synthesis and characterization of Fe₃O₄@ TiO₂ for drug delivery applications” is solely my research work with no significant contribution from any other person. Small contribution/ help wherever taken has been duly acknowledged and that complete thesis has been written by me.

I understand the zero-tolerance policy of the HEC and National University of Sciences and Technology (NUST), Islamabad towards plagiarism. Therefore, I as an author of the above titled thesis declared that no portion of my thesis has been plagiarized and any material used as reference is properly referred/cited.

I undertake that if I am found guilty of any formal plagiarism in the above titled thesis even after award of MS degree, the University reserves the rights to withdraw/revoke my MS degree and that HEC and NUST, Islamabad has the right to publish my name on the HEC/University website on which names of students are placed who submitted plagiarized thesis.

Student Signature:



Name: Anum Rabab

DEDICATION

I dedicate this thesis to My Father & My Respected Teachers without whom I would not be here. Thanks for their endless Guidance and Support.

ACKNOWLEDGEMENTS

All glories belong to almighty ALLAH, the most beneficent and merciful, who conferred us with good health, caliber, and awareness to achieve our ambition. First, I pay my heartiest thanks to my supervisor **Dr. I.H GULL**, who helped me to the maximum level to achieve my goal. Despite his tough routine, he was always ready to help me in all the difficult situations or any type of discussion. His doors were always open for notable discussions, and implications with remarkable hospitality. I am also thankful to my GEC members Dr Zakir Hussain, Dr Nasir Ahmed, Dr Usman Liaqat, other academic staff and all staff members of the Department of SCME, NUST, Islamabad, for their help in academic matters as well as research facilities throughout MS program.

I was exceptionally lucky to have numerous great companions and associates like Ibrahim Siddiqui, M. Zafar Khan, Hina Maqsood and Varda Shakeel here at SCME NUST. I express my genuineness because of every one of them for their welcoming collaboration and support.

I feel short of words while expressing my gratitude to my loving FATHER and my siblings for their love and wish to see me shining high on the skies of success.

TABLE OF CONTENTS

| | |
|---|-------------|
| ACKNOWLEDGEMENTS | viii |
| TABLE OF CONTENTS | ix |
| LIST OF FIGURES | xii |
| LIST OF TABLES | xiv |
| LIST OF ABBREVIATIONS | xv |
| ABSTRACT | xvi |
| CHAPTER 1: INTRODUCTION | 1 |
| 1.1 Notion of Nano technology: | 1 |
| 1.2 Magnetism | 1 |
| 1.2.1 Magnetism and its types | 2 |
| 1.3 Ferrites | 6 |
| 1.3.1 Categorization of ferrites | 6 |
| 1.3.2 Types of ferrites | 7 |
| 1.3.3 Applications of Ferrites | 10 |
| 1.4 Magnetic Nano Particles (MNPs): | 10 |
| 1.5 Preparation of Nanoparticles | 13 |
| 1.5.1 Physical Methods | 13 |
| 1.5.2 Physical Vapor Deposition (PVD)/Chemical Vapor Deposition (CVD): | 13 |
| 1.5.3 Chemical Methods | 15 |
| 1.5.3.5 Sono-Chemical Synthesis | 16 |
| 1.5.4 Biological Methods | 16 |
| 1.6 Drug Delivery applications of MNP..... | 18 |
| 1.7 Research Goal | 20 |
| 1.8 Aim of study | 20 |
| CHAPTER 2: LITERATURE REVIEW | 21 |
| 2.1 Iron Oxide Nanoparticles:..... | 21 |
| 2.2 Surface Modification of Iron Oxide Nanoparticles: | 22 |
| 2.3 Iron Oxide Based Drug Delivery: | 23 |
| 2.4 TiO ₂ Applications in Biomedicine:..... | 29 |

| | |
|---|-----------|
| 2.5 TiO ₂ Applications in the Field of Drug Delivery: | 30 |
| CHAPTER 3: MATERIALS & METHODS..... | 32 |
| 3.1 Synthesis technique for nanomaterials: | 32 |
| 3.1.1 Top-down approach | 32 |
| 3.1.2 Bottom-Up approach..... | 33 |
| 3.1.2.1 Sol gel method | 33 |
| 3.1.2.2 Coprecipitation Method | 34 |
| 3.1.2.3 Hydrothermal Method..... | 35 |
| 3.2 Synthesis of Fe ₃ O ₄ @TiO ₂ :..... | 37 |
| 3.2.1 Materials: | 37 |
| 3.2.1.1 Synthesis of Fe ₃ O ₄ | 37 |
| 3.2.2 Synthesis of TiO ₂ :..... | 38 |
| 3.2.3 Synthesis of Fe ₃ O ₄ @TiO ₂ nanoparticles:..... | 39 |
| 3.3 Drug Loading on Nanoparticles:..... | 40 |
| 3.4 Drug Release Study: | 40 |
| 3.5 Hemolysis Assay: | 40 |
| 3.6 UV -Vis Spectroscopy | 40 |
| CHAPTER 4: CHARACTERIZATION TECHNIQUES | 41 |
| 4.1 X-Ray Diffraction Technique:..... | 41 |
| 4.1.1 Working Principle of XRD | 42 |
| 4.1.2 Crystal Structure | 43 |
| □ Laue Method | 43 |
| □ Rotating Crystal Method..... | 43 |
| □ Powder Method..... | 43 |
| 4.1.3 Lattice Constant | 44 |
| 4.1.4 Crystallite size..... | 45 |
| 4.2 Scanning Electron Microscopy: | 45 |
| 4.2.1 Fundamental SEM Principle..... | 46 |
| 4.3 Fourier-Transform Infrared Spectroscopy (FTIR) | 47 |
| 4.3.1 Working Principle of FTIR..... | 47 |
| 4.4 UV Vis Spectroscopy: | 48 |
| 4.5 Hemolysis Testing: | 50 |
| 4.5.1 Working Principle of Hemolysis Assay..... | 50 |

| | |
|---|-----------|
| CHAPTER 5: RESULTS & DISCUSSION | 52 |
| 5.1 XRD Analysis: | 52 |
| 5.2 Scanning Electron Microscopy | 54 |
| 5.2.1 Fe ₃ O ₄ | 54 |
| 5.2.2 SEM of Fe ₃ O ₄ @TiO ₂ | 55 |
| 5.3 FTIR:..... | 57 |
| 5.4 Drug Loading of Nanoparticles | 59 |
| 5.4.1 Standard Curve of ciprofloxacin:..... | 59 |
| 5.5 Drug loading on Nanoparticles:..... | 60 |
| 5.6 Drug Release Studies of Nanoparticles | 61 |
| 5.7 Hemolysis Assay..... | 63 |
| CHAPTER 6: CONCLUSION | 65 |
| REFERENCES: | 66 |

LIST OF FIGURES

| | |
|---|----|
| Figure 1.1.1: Schematic of diamagnetism..... | 3 |
| Figure 1.2: Schematics of paramagnetism | 3 |
| Figure 1.3: Alingment of magnetic dipole moment of ferromagnetic materials | 4 |
| Figure 1.4: Ferrimagnetic materials domain..... | 5 |
| Figure 1.5: Anti-Ferromagnetic domains..... | 5 |
| Figure 1.6: Superparamagnetic materials behaviour, Hysteressis loop | 6 |
| Figure 1.7: Classification of ferrites | 7 |
| Figure 1.8: Crystal structure of spinal ferrite..... | 9 |
| Figure 3.1: Schematics of top -down and bottom-up approach..... | 32 |
| Figure 3.2: Schematic of sol-gel process | 34 |
| Figure 3.3: Flow chart of coprecipitation method | 35 |
| Figure 3.4: Hydrothermal process..... | 35 |
| Figure 3.5: Micro emulsion process..... | 36 |
| Figure 3.6: Hydrothermal synthesis process of Fe_3O_4 | 38 |
| Figure 3.7: Hydrothermal synthesis of TiO_2 | 39 |
| Figure 3.8: Synthesis of TiO_2 coated Fe_3O_4 nano particles | 39 |
| Figure 4.1:Experimental setup of XRD technique..... | 42 |
| Figure 4.2: Incident x-ray beam scattered by atomic plane in a crystal | 43 |
| Figure 4.3: Debye scherre cones produced by crystallized material powder and a mono chromatic x-ray beam | 44 |
| Figure 4.4: (a) Experimental setup of SEM ,(b) Different rays reflected from incident beam..... | 46 |
| Figure 4.5: FTIR setup..... | 48 |
| Figure 4.6: Components of UV-Vis spectroscopy..... | 48 |

| | |
|--|----|
| Figure 4.7: Path that UV light takes to pass through reference and sample cuvette.... | 49 |
| Figure 4.8: Schematic of hemolysis assay | 50 |
| Figure 5.1: XRD pattern of Fe ₃ O ₄ and Fe ₃ O ₄ @ TiO ₂ with wt.% (5, 10, 15, 20)..... | 54 |
| Figure 5.2: SEM of Fe ₃ O ₄ | 55 |
| Figure 5.3: SEM of Fe ₃ O ₄ @ TiO ₂ (b) 5% (c) 10% (d) 15% (e) 20% | 56 |
| Figure 5.4: FTIR analysis (a) Fe ₃ O ₄ (b) Fe ₃ O ₄ @ TiO ₂ (5%) (c) Fe ₃ O ₄ @ TiO ₂ (10%) (d) Fe ₃ O ₄ @ TiO ₂ (15%) (e) Fe ₃ O ₄ @TiO ₂ (20%)..... | 58 |
| Figure 5.5: Linear curve of ciprofloxacin | 59 |
| Figure 5.6: Encapsulation efficiency of Fe ₃ O ₄ and Fe ₃ O ₄ @ TiO ₂ (5%, 10%, 15%, 20%)..... | 61 |
| Figure 5.7: Cumulative drug release of Fe ₃ O ₄ and Fe ₃ O ₄ @ TiO ₂ (5%, 10%, 15%, 20%)..... | 62 |
| Figure 5.8: Fe ₃ O ₄ , Fe ₃ O ₄ @ TiO ₂ and drug loaded Fe ₃ O ₄ @TiO ₂ | 64 |

LIST OF TABLES

| | |
|--|----|
| Table 1 . Summary of Nanomaterials with properties favorable to biomedical applications | 12 |
| Table 2. Summary of pros and cons of nanoparticles' synthesis techniques..... | 17 |
| Table 3. TiO ₂ applications summary in biomedical field | 31 |
| Table 4. Crystallite size and lattice constant of Fe ₃ O ₄ and Fe ₃ O ₄ @TiO ₂ | 53 |
| Table 5. Absorbance values of ciprofloxacin with different concentrations. | 59 |
| Table 6. Encapsulation efficiency (%) of Fe ₃ O ₄ and Fe ₃ O ₄ @TiO ₂ loaded with Ciprofloxacin | 60 |

LIST OF ABBREVIATIONS

| | |
|---------------|---|
| SEM | Scanning Electron Microscope |
| XRD | X-ray Powder Diffraction |
| FTIR | Fourier-Transform Infrared Spectroscopy |
| SPIONs | Superparamagnetic Iron Oxide Nanoparticles |
| nm | Nanometers |
| BIM | Biologically Induced Biomineralization |
| BCM | Biologically Controlled Biomineralization |
| CVD | Chemical Vapor Deposition |
| PVD | Physical Vapor Deposition |
| MNPs | Magnetic Nanoparticles |
| RES | Reticuloendothelial System |
| MRI | Magnetic Resonance Imaging |
| NSAID | Non-Steroidal Anti-Inflammatory Drugs |
| DMSO | Dimethyl Sulfoxide |
| HMEM | Hank's Minimum Essential Medium |
| EE | Encapsulation Efficiency |
| CC | Cumulative Concentration |

ABSTRACT

Drug delivery systems have substantially advanced as an outcome of the medical field's utilization of nanotechnology. $\text{Fe}_3\text{O}_4@\text{TiO}_2$ core-shell nanoparticles, which combine the biocompatibility of TiO_2 with the magnetic characteristics of Fe_3O_4 (magnetite), are an intriguing method. This study focusses on using hydrothermal synthesis to generate $\text{Fe}_3\text{O}_4@\text{TiO}_2$ nanoparticles for targeted drug delivery applications. The model drug deployed was ciprofloxacin and it was intended to be loaded onto Fe_3O_4 nanoparticles that were both pure and TiO_2 -incorporated. The structural, morphological, and functional group attributes were explored by employing XRD, SEM, and FTIR correspondingly. XRD evaluation revealed the unique peaks of both components, confirming the successful formation of Fe_3O_4 and $\text{Fe}_3\text{O}_4@\text{TiO}_2$ core-shell nanoparticles. The particle size of these nanoparticles was less than 100 nm, making them appropriate for use in biological applications, according to SEM analysis. The effective synthesis and functionalization of the nanoparticles were validated by FTIR, which also indicated the presence of functional groups. The hemolysis assay and drug loading and release features were studied using UV-Vis spectroscopy. $\text{Fe}_3\text{O}_4@\text{TiO}_2$ nanoparticles with a weight percentage of 20 shown to have the highest drug encapsulation efficiency and greatest drug release, pursuant to the findings. With an initial burst release over the first 4 hours, the total drug release over the course of 24 hours was 93.21%. As the TiO_2 content boosted the hemolytic activity of the $\text{Fe}_3\text{O}_4@\text{TiO}_2$ nanoparticles minimized implying enhanced biocompatibility. Hemolytic activity of 4.6% was obtained with a TiO_2 Wt % 20, suggesting low toxicity and excellent blood compatibility. Their performance and biocompatibility can be further improved by adjusting the Fe_3O_4 to TiO_2 ratio, opening the door for their employment in cutting-edge therapeutic applications.

CHAPTER 1: INTRODUCTION

1.1 Notion of Nano technology:

Nanotechnology is one of the most important fields of study in modern science as it empowers scientists, engineers, and researchers to operate at the molecular and cellular level. Whenever it comes to features, organic or inorganic materials with at least one size dimension between 1 and 100 nanometers (nm) are known as nanoparticles. These materials have better qualities than their bulk counterparts. [1], have enhanced properties as compared to their bulk counterparts. Nano materials are basically divided with respect to their dimension including zero dimensions characterized as quantum dots, one dimension as wires and rods at nano scale, two dimensional nano materials include nano films, nanolayers and nanocoating like graphene and three dimensions includes belts, sheets, disks and films at nanoscale. Due to their superior optical, catalytic, electric and magnetic properties nanoparticles are getting great attention. Nanoparticles in such size range are faster, lighter in weight, can get into smaller spaces, cheaper and are more energy efficient. Nanoparticles at this size range enhance adsorption, absorption and penetration due to improved interaction at molecular level. The changes in properties at nanoscale are due to two main reasons. Firstly, the surface area to volume ratio increases as most of the atoms become nearer to the surface hence making them weakly bonded and makes them more reactive. Secondly there is a change in electric and optical properties of the material which in due to quantum mechanical effect in which size of the structure become relatable to the wavelength of the electron which results in quantum confinement and hence change in optical and electronic properties can be seen. Due to these reasons, we can see enhanced properties like reduce in melting point, increase in hardness, changed optical, electrical and magnetic properties, self-purification process can be seen and due to increase in perfection chemical stability can be seen. Due to excellent properties of these nanoparticles an unusual increase in their use in life sciences can be seen. In the field of biomedicine nanotechnology has introduced various applications. Including targeted drug delivery, magnetic hyperthermia, Bio imaging, sensors (bio sensors) and many other applications. Nano technology majorly focuses on therapeutic and diagnostic applications in the field of biomedical science as done in past researches[2-4].

1.2 Magnetism

Magnetic nanoparticles can be manipulated using external magnetic field as their properties are strongly anchored by the morphology, size, surface functionalities and magnetization values. The magnetic nature of nanoparticles is characterized by their electrostatic forces produced by orbital and spinning motion of electrons and their interactions. The response of a material to a magnetic field is known as magnetic susceptibility meaning how much a material is magnetized in presence of a magnetic field. The ability of a material to retain magnetism in the absence of magnetic field is known as remanence and the total amount of magnetization required to completely demagnetize the magnetic material is known as coercivity.

Magnetic materials are characterized based on their magnetic moment's magnetic susceptibility and orientation which are described below.

1.2.1 Magnetism and its types

Magnetism arises by the orbital and spin motions of the electrons as well as their interactions with one another. These variants show how magnetic materials respond to an external magnetic field [5]. There are different kinds of magnetic materials according to the external applied field

- Diamagnetic
- Paramagnetic
- Ferromagnetic
- Ferrimagnetic
- Anti ferromagnetic
- Super paramagnetic

1.2.1.1 Diamagnetic Material:

These are the materials when placed under an external magnetic field they get weakly repelled by that magnetic field and get magnetized in the opposite direction of applied magnetic field having weak and negative susceptibility value. When placed in a magnetic field the magnetic field lines are repelled from the center of diamagnetic material. When placed under nonuniform field the diamagnetic material moves from strong field region

to weak field region. This material loses magnetization when external magnetic field is removed due to no unpaired electrons. These materials could be in the form of water liquid and gas. Examples include hydrogen, mercury, water, copper, and gold.

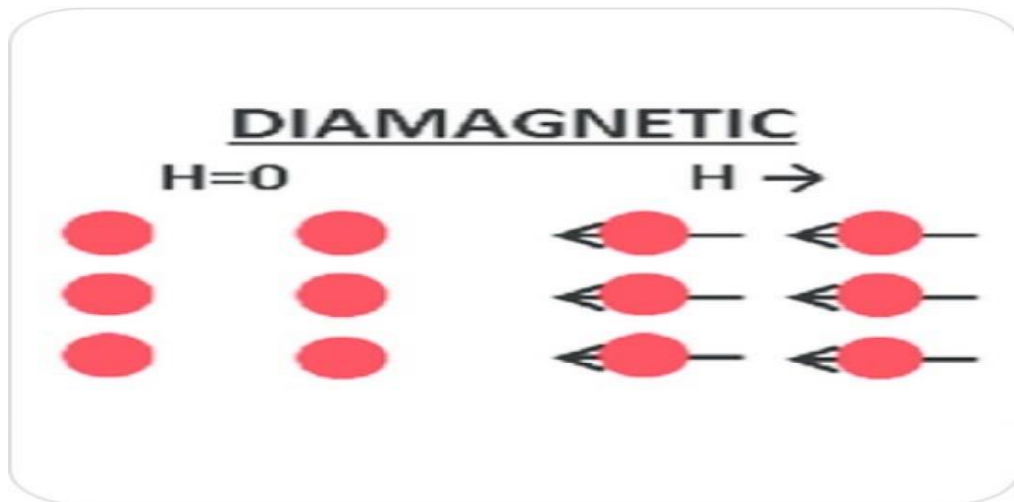


Figure 1.1.1: Schematic of diamagnetism

1.2.1.2 Paramagnetic Material

These are the materials when placed under external magnetic field they get weakly attracted by that magnetic field and get magnetized in the same direction of applied magnetic field having weak and positive susceptibility value. When placed in a magnetic field the magnetic field lines are attracted to the center of Paramagnetic material. When placed under a nonuniform field the paramagnetic material moves from weak field region to strong field region. This material loses magnetization when the external magnetic field is removed but has some unpaired electrons. These materials could be in the form of water liquid and gas. Examples include Aluminum, platinum, sodium and crown glass.

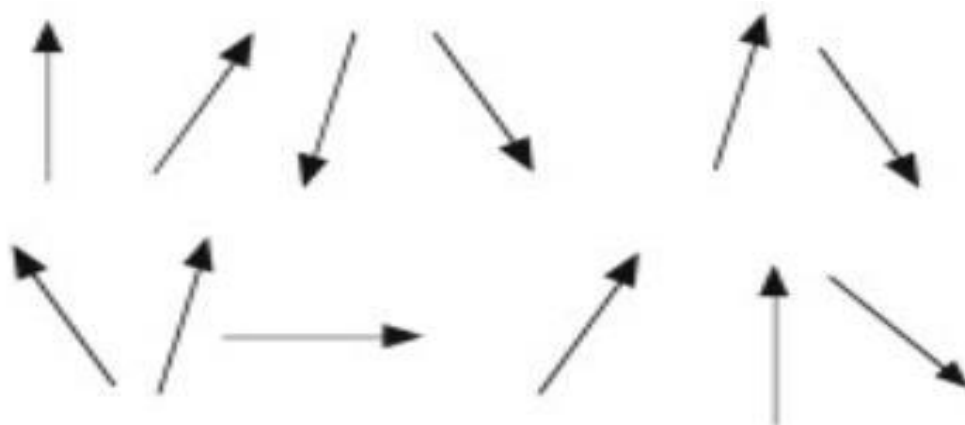


Figure 1.2: Schematics of paramagnetism

1.2.1.3 Ferromagnetic Material:

These are the materials when placed under external magnetic field they get strongly attracted by that magnetic field and get magnetized in the same direction of applied magnetic field having strong and positive susceptibility value. When placed in a magnetic field the magnetic field lines are strongly attracted to the center of ferromagnetic material. When placed under a nonuniform field the ferromagnetic material moves from weak field region to strong field region. These materials retain magnetization when the external magnetic field is removed and can act as a magnet and have unpaired electrons. These materials could only be in the form of gas. Examples include iron, cobalt and nickel.

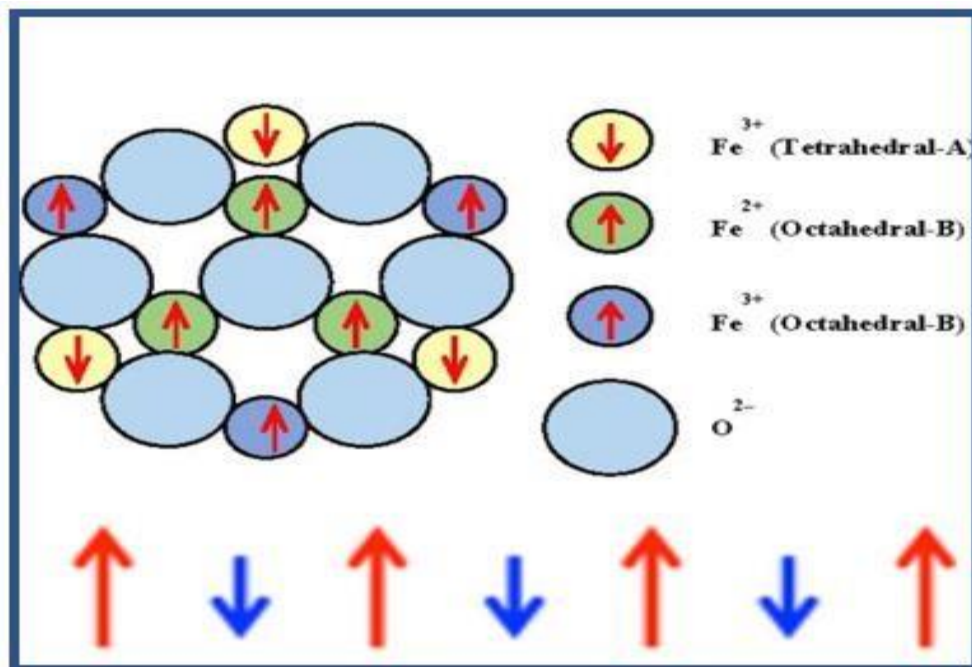


Figure 1.3: Alingment of magnetic dipole moment of ferromagnetic materials

1.2.1.4 Ferrimagnetic Material:

These are the materials in which magnetic domains are aligned in both parallel and anti-parallel direction in unequal numbers, so they are unable to cancel out each other. This occurs as the sublattices are separated by oxygen ions. These materials are weakly attracted by magnetic fields. Examples include Fe_3O_4 , MgFe_2O_4 , ZnFe_2O_4 etc. These materials sometimes lose their ferrimagnetic property and change to paramagnetic material.

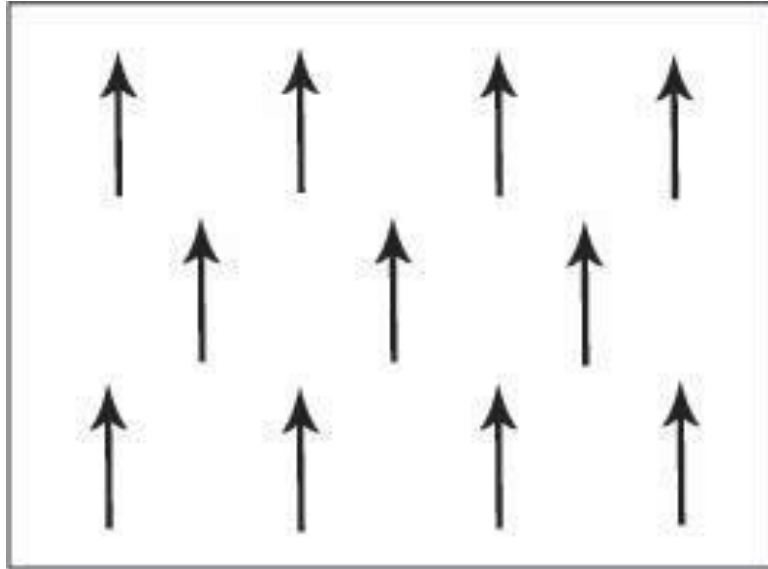


Figure 1.4: Ferrimagnetic materials domain

1.2.1.5 Anti-Ferromagnetic Material

In this type of material adjacent dipoles are arranged in anti-parallel manner with same magnitude. Susceptibility is very small and positive, and it is usually dependent on temperature. The susceptibility increases until the Neel temperature and after that susceptibility decreases. Examples of these materials are MnO, MnS, Cr₂O₃ and NiCr etc.

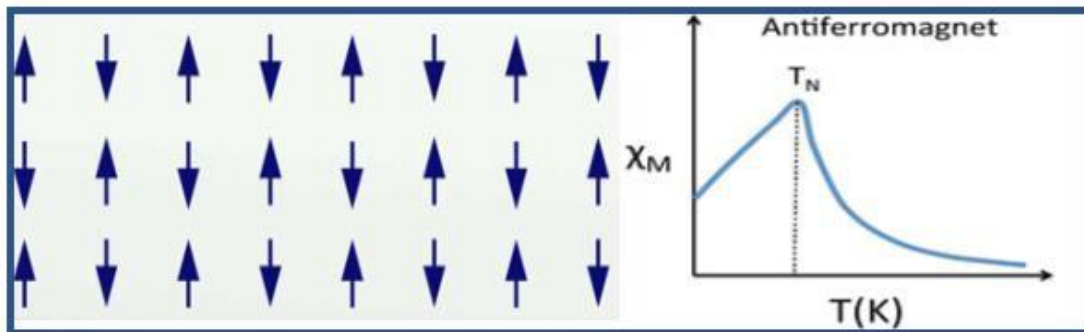


Figure 1.5: Anti-Ferromagnetic domains

1.2.1.6 Super Para Magnetic Material:

The phenomenon of superparamagnetic occurs when the particle size is below a critical particle size below which particle have single domain making them superparamagnetic. In this size materials coercivity, remanence and hysteresis become zero. The logic behind this is that as the particle size decreases the anisotropy energy decreases which results in decrease in

coercivity. As the size decreases volume dependent anisotropy decreases and becomes comparable to thermal energy and time come when thermal energy become greater which eventually results in flipping of magnetization with high frequency form one direction to another even in the absence of magnetic field which results in the phenomenon of superparamagnetic[6].

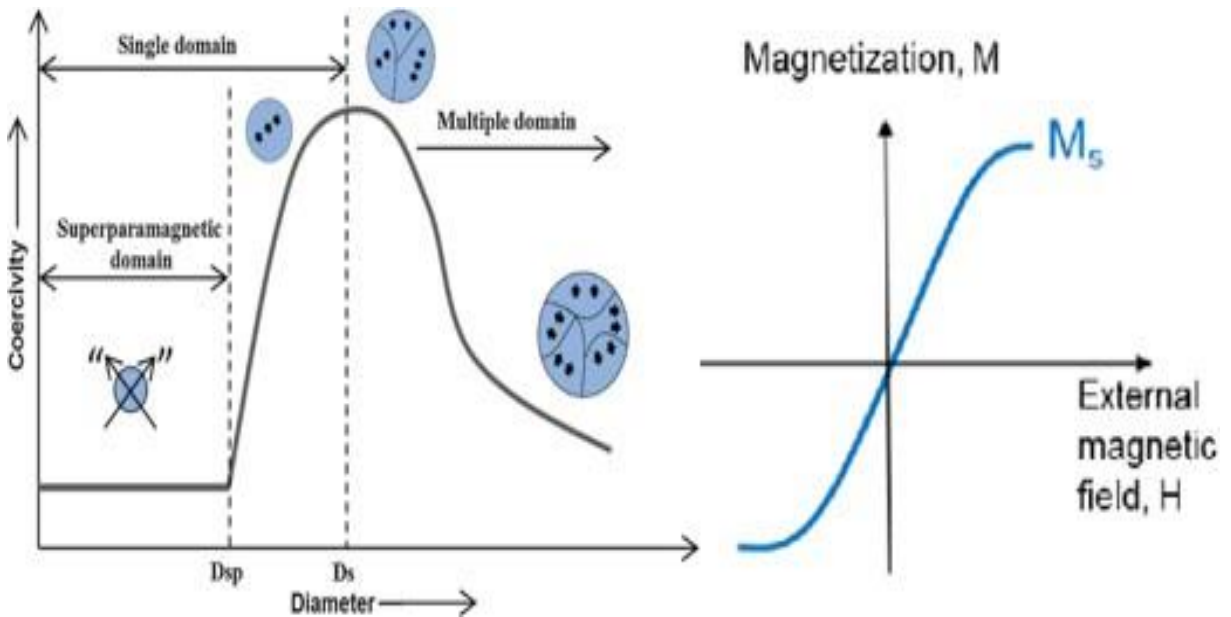


Figure 1.6: Superparamagnetic materials behaviour, Hysteresis loop

1.3 Ferrites

The most important class of magnetic minerals are ferrites, which are used for a variety of purposes. They can be used in transformers, memory chips, antenna rods, inductors, and other devices. They have recently been used in sensors, green anode materials, and medication delivery. The three most important properties of ferrite are low dielectric losses, low eddy current, and high electrical resistivity. Ferrites are widely used in computers, microwaves, high frequencies, and magnetic freezers [7].

1.3.1 Categorization of ferrites

Ferrites can be categorized into two main groups owing to their distinct characteristics and wide range of uses.

- Soft ferrites
- Hard ferrites

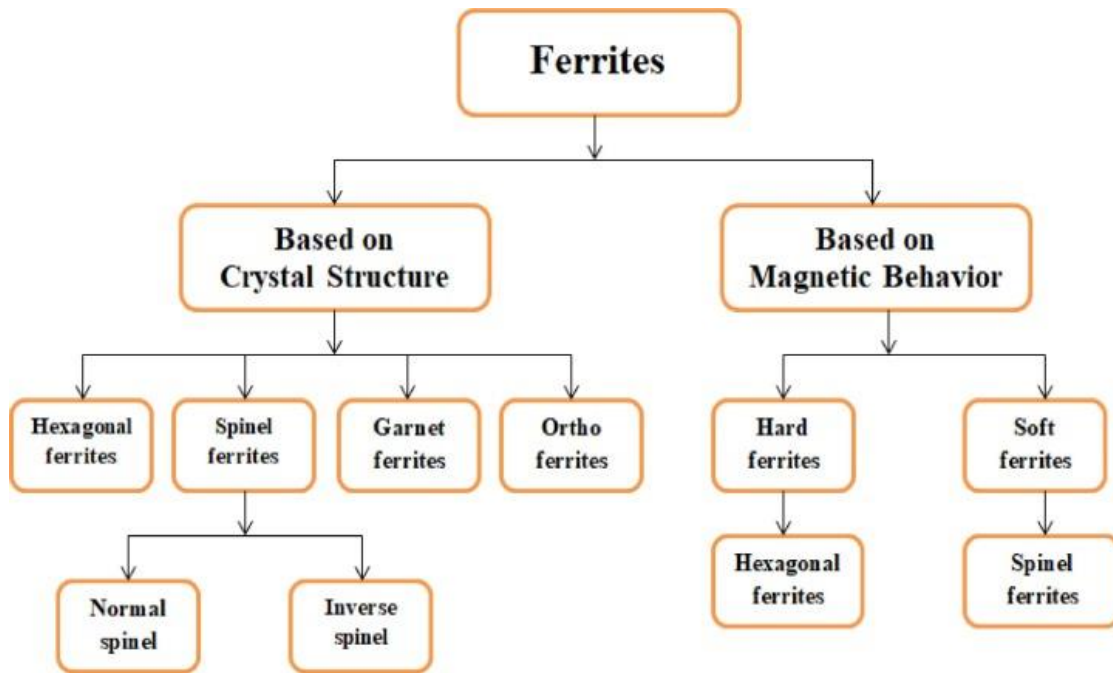


Figure 1.7: Classification of ferrites

1.3.1.1 Soft Ferrites

Soft ferrites are easily magnetized and demagnetized by exposing them to an applied field. They will only stay magnetized in the presence of a magnetic field. Soft ferrites have very low coercivity and hysteresis loops, suggesting that the material's magnetization may change direction quickly and with little energy expenditure [8].

1.3.1.2 Hard Ferrites

Hard ferrites retain their material or magnetization after the applied field is removed. They have high amounts of hysteresis loops and coercivity. Hard ferrites are the behavior shown by iron oxides, barium oxides, and strontium oxides. Hard ferrites are composed of iron and oxides of strontium or barium. They can withstand magnetic fields stronger than those of iron because of their high magnetic permeability [9].

1.3.2 Types of ferrites

There are two types of ferrites

- Cubic shaped ferrites
- Hexagonal shaped Ferrites

1.3.2.1 Cubic ferrites

Cubic ferrites are divided into two types

- Spinel ferrites
- Garnet ferrites

1.3.2.1.1 Spinel ferrites

With tetrahedral [A] and octahedral [B] sites, spinel ferrites have the chemical formula $M\text{Fe}_2\text{O}_4$, where M=divalent metal ion. Both tetrahedral A site and the octahedral B site's properties change when cations are present. If other metal ions are used in place of divalent M, a significant number of spinel ferrites will result. Other trivalent ions such as Al^{3+} , Cr^{3+} , Ga^{3+} , etc., or a combination of divalent and tetravalent ions are used to replace iron ions (Fe^{2+}). These ferrites have flexibility. Low magnetic loss and high electrical resistance are characteristics of spinel ferrites [10].

These materials are stable and magnetic. Spinel ferrites (SFs) typically have the chemical formula $M\text{Fe}_2\text{O}_4$, where M stands for Co, Fe, Mn, Ni, Cu, and Zn. These ferrites have the same cubic symmetry as the mineral spinel. SFs are super paramagnetic (SPM) at the nanoscale, with a diameter of less than or equal to 20 nm. Spinel ferrite nanomaterials have unique properties and use in a range of applications such as elevated densities for gas sensors, catalysts, and data storage; rechargeable batteries, such lithium batteries, for medical diagnosis and treatment; magnetic bulk cores; magnetic fluids; microwave absorbers; data storage systems; etc. [11].

Crystal structure of Spinel Ferrite

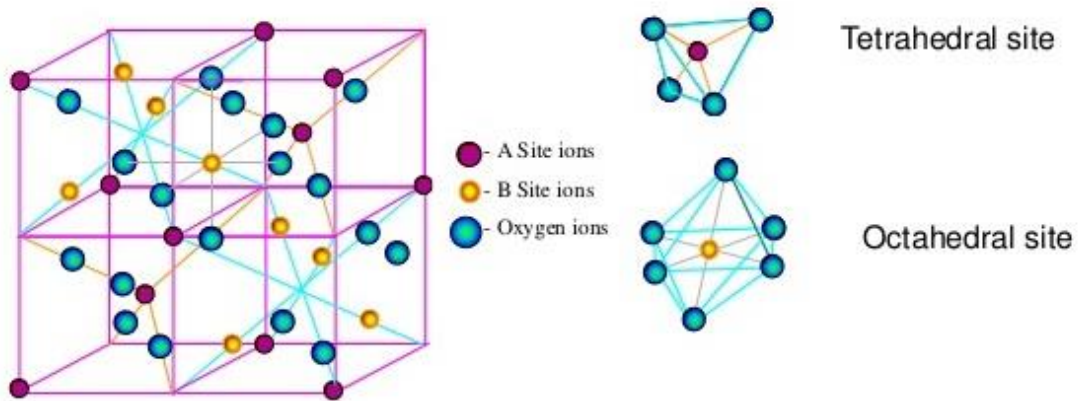


Figure 1.8: Crystal structure of spinel ferrite

1.3.2.1.1.1 Types of Spinel ferrites

Spinel ferrites are divided into three types

- Inverse spinel ferrites

In this instance, half of the octahedral sites are occupied by the divalent cations (A), and all the additional octahedral sites and all the tetrahedral sites are occupied by the trivalent cations (B). Magnetite (Fe_3O_4) is a common example, where the distribution of iron cations is as outlined.

- Normal spinel ferrites

The octahedral positions in these ferrites are taken up by trivalent iron cations (B) and the tetrahedral sites by divalent metal cations (A). Zinc ferrite is one such example (ZnFe_2O_4).

- Mixed spinel ferrites

Divalent and trivalent cations are dispersed randomly throughout the tetrahedral and octahedral sites of these ferrites. By modifying the cation distribution, this specific type of spinel can be made to have characteristics. Cobalt ferrite (CoFe_2O_4) and nickel ferrite (NiFe_2O_4) are two examples.

1.3.2.1.2 Garnet Ferrites

The garnet was discovered in 1957 by Geller and Gilleo. Eight formula units of $M_3Fe_5O_{15}$, where M is a trivalent rare earth ion like Y, Gd, or Dy, are found in the unit cell of a pure iron garnet. Ferrites are unique translucent ceramics with a magnetic field. In magneto optical technology, they are useful. Garnet ferrites are composed of three sub-lattices. There are eight formula units, or 160 atoms, in a cubic unit cell. The edges of the cubic cell measure roughly 12.5Å in length. Three interstices are occupied by metal cations in an array of 96 oxygen ions [12].

1.3.2.2 Hexagonal Ferrites

They are widely used as permanent magnets and have strong coercive properties that first became known in 1952. Hexagonal ferrites have a significant uniaxial magneto crystalline anisotropy, which makes them useful in permanent, hard magnets. The letters M, W, Y, and Z stand for four distinct types of hexagonal ferrites with the general formula $MO_6Fe_2O_3$. M could be Pb, Sr, or Ba. They are hard ferrites because it is difficult to simply reverse the direction of magnetization [13].

1.3.3 Applications of Ferrites

Ferrites' high resistance, higher magnetism properties, inexpensiveness, and ease of fabrication make them ideal magnetic materials compared to pure metals.

Some uses for ferrites are listed below

- High density optical recordings
- Pollution control
- Magnetic sensors
- Drug delivery
- Magnetic shielding
- Supercapacitors
- Ferrites electrodes.

1.4 Magnetic Nano Particles (MNPs):

Applications of MNPs are growing faster nowadays. Having size ranging from 1nm to 100 nm, these nanoparticles are distinguishable from their bulk counterpart. The characteristics of MNPs, particularly their high surface area, high magnetization values, metal-enriched

constituents, chemical stability, surface functionalization capability, molecular and cellular application, and biocompatibility, make them ideal for a range of applications in the biomedical industry. Properties of MNPs can be controlled by changing their physiochemical properties and can be applied to various fields. The size and shape of nanoparticles depends on the synthesizing conditions such as surfactants, temperature etc. crucial for the synthesis of mono dispersed nature. These nanoparticles can be used in applications like biomedicine, environmental fields and agriculture. MNPs are made up of different metal elements and metal oxides having magnetic properties. The composition of nanoparticles can be comprised of different types including mono- components comprising of nanoparticles based on Fe, Ni and Co having good magnetic properties[14]. In these nanoparticles iron is mostly studied due to its chemical stability, biocompatibility and environmentally friendly nature, metal alloys based nanoparticle including Iron platinum (FePt) and Iron palladium (FePd) nanoparticles having high magnetic crystallinity and chemical stability, metal oxide based nanoparticles majorly comprising of magnetite nanoparticles having high magnetization values, biocompatibility and chemical stability[15], metal carbides nanoparticles comprising of nanoparticles based on iron carbide including Fe₅C₂, Fe₃C and Fe₂C. It also includes hetero-structure magnetic nanoparticles containing nanostructure like FePt-Au magnetic structures which exhibits excellent magnetic properties[16]. Majorly Iron oxide nanoparticles are used in biomedical application due to their superior properties like high magnetic saturation, good stability and minimal toxicity. Maghemite ore of iron oxide is more stable in aqueous media give more magnetic character. Iron oxide nanoparticle of size above 50 nm is known as superparamagnetic and whereas below 50nm it is known as ultra-small superparamagnetic. Magnetic ferrites having general formula of MFe₂O₄, having spinal structure, are extensively studied due to their biomedical applications. The 'M' in the MFe₂O₄ represents material like Zinc, Manganese, Cobalt, Nickel and magnesium etc.[17]. The magnetic characteristics of iron oxide's magnetic core are enhanced by these compounds.

Cobalt or magnesium doping helps to improve the magnetic characteristics of iron oxide by increasing specific absorption rate and magnetic resonance signals, respectively[15, 18]. Some of these nanoparticles with their biomedical applications are given below in table 1.

Table 1 . Summary of Nanomaterials with properties favorable to biomedical applications

| Material Category | Nano Particles | Properties |
|--------------------------|---------------------------------------|--|
| Metallic | Gold (Au) | <ul style="list-style-type: none"> • Chemical inertness • Ability of surface functionalization • Negative charge on its surface |
| | Silver (Ag) | <ul style="list-style-type: none"> • High electrical conductivity • Thermal conductivity • Chemical stability • Catalytic activity • Antibacterial • Enhanced optical properties |
| Bi-Metallic | FePt | <ul style="list-style-type: none"> • Chemical stability • super Para magnetization • High Curie temperature • High saturation magnetization • High X-ray absorption |
| | FeCo | <ul style="list-style-type: none"> • Super Para magnetism • High Curie temperature • High saturation magnetization |
| | FeNi | <ul style="list-style-type: none"> • High Curie temperature • High saturation magnetization |
| | CuNi | <ul style="list-style-type: none"> • Good Curie temperatures • Magnetic properties |
| Magnetic | Fe₃O₄ | <ul style="list-style-type: none"> • Chemical Stability • Nontoxicity • Biocompatibility • High saturation magnetization • High magnetic susceptibility |
| | Co-Fe₂O₄ | <ul style="list-style-type: none"> • High magneto-crystalline anisotropy • High coercivity • High curie temperature • Moderate magnetization saturation • Chemically stable |
| | Mn-Fe₂O₄ | <ul style="list-style-type: none"> • High magnetization • Magnetic susceptibility • Large relativities • Biocompatible. |

1.5 Preparation of Nanoparticles

Nano particles can be synthesized using various techniques. These techniques can be divided into three major categories including physical, chemical and biological methods[19].

In physical methods we synthesize nanoparticles using techniques like gas phase deposition, pulse laser ablation, electron beam lithography, laser induced pyrolysis and power ball milling techniques. Chemical methods include techniques like co-precipitation, micro-emulsion, hydrothermal and sol gel methods. Biological methods include green synthesis of nanoparticles using bacteria fungi or protein extracts. The method is chosen based on desired shape, size, distribution, purity and quantity of end nano-product. The following details of synthesis include:

1.5.1 Physical Methods

Within the field of nanotechnology, a physical method comprises methods and procedures that generate, engage with, and alter nanoparticles and nanostructures using physical forces and principles. Usually, mechanical, thermal, or electromagnetic forces are used in place of chemical reactions in these techniques to produce the required nanoparticle properties. Physical techniques are frequently chosen because they may yield very pure nanoparticles with exact control over size and structure.

1.5.2 Physical Vapor Deposition (PVD)/Chemical Vapor Deposition

(CVD):

PVD and CVD are basically part of gas phase deposition technique in which the particles are supersaturated from gas phase onto the substrate. The process is done in an inert atmosphere which leads to the production of fine powders or thin films without any contamination. The precursors are evaporated in a chamber filled with inert gas and at higher atmospheric pressure. The precursors collide with inert gas and lose their energy hence condensing into nanocrystals through the phenomenon of Brownian gelling and combination[20]. The particles produced through gas phase are much pure and there is no contamination as compared to liquid phase deposition technique[21]. Through this technique the particles can be synthesized on bulk scale. The drawback of this technique is that the size of the nanoparticles cannot be maintained throughout the experiment.

1.5.2.1 Electron Beam Lithography:

In this technique a beam of electron is emitted on a substrate of the material whose nanoparticulate are desired. The emitted electron beam removes the exposed or non-exposed area of the substrate surface which is usually immersed in a water bath which evaporates the material creating nanoparticle below 50 nm of size[21]. This technique gave us small size nanoparticles but consist of disadvantages like high production cost and having long process time making it uneconomical.

1.5.2.2 Pulse Laser Ablation:

In this technique conditions like temperature, pressure, density etc. can be controlled effectively with respect to other physical methods. In this process the material is removed from the target using a pulse laser beam. This process produces a plasma cloud at higher temperature and pressure which reacts with the ablated material to form metastable nanoparticle through the course of nucleation and growth. The positive aspect of this process is that it is environmentally friendly as no harm to the environment by the byproduct formed. Despite having many positive aspects, the process has drawbacks like sputtering and inhomogeneity in the energy profile of the plume[22-24].

1.5.2.3 Pyrolysis Induced By laser:

In this process a laser is used to heat a gaseous mixture of precursors of nanoparticles which produces scattered nanoparticles[25]. In this process the parameters are varied like fuel to air ratio and vapor pressure of the precursors which produces nanoparticles in size below 7 nm[26]. The techniques have a drawback of difficulty in controlling size of final particles therefore we get a broad range of size distribution of these nanoparticles.

1.5.2.4 Ball Milling:

In this method the precursor powder is milled in a jar with the help of metallic balls (e.g. Tungsten carbide balls). The phenomenon of cold welding and fracture occurs during the whole process and fine and uniformly dispersed powder is obtained. The size highly depends upon mills rotation time and speed. Industrial scale production of nanoparticles is possible through ball milling technique[27, 28]. Agglomeration is a drawback of this technique which can be overcome by using surfactants or ultrasonication of particles[28].

1.5.3 Chemical Methods

An approach or procedure used in nanotechnology to create, work with, and alter nanoparticles and nanostructures is referred to as a chemical method. These techniques usually entail the controlled synthesis and functionalization of nanoparticles using chemical precursors, solvents, and reagents. Chemical techniques are extensively employed due to their capacity to generate nanoparticles with dimensions, forms, and surface characteristics, frequently at comparatively low temperatures and in moderate environments.

1.5.3.1 Co-precipitation

It is the process in which precursors are reduced using a reducing agent and nanoparticles are obtained under the condition of super saturation. It is the simplest and most widely used technique for the synthesis of nanoparticles. It includes the collective existence of nucleation, growth and coarsening. Nucleation is the key step in this process. In this technique nano sized particles are precipitated out of a continuous solvent. Metallic salts that are inorganic in nature are dissolved in a solvent. These metallic salts act as metal hydrates species which are reduced by a basic solution creating a condition of super saturation and nanoparticles are precipitated out. Change in pH, ionic strength and amount of reducing agent can be used to control particle size and shape[29, 30].

1.5.3.2 Hydrothermal Technique:

It is a process in which reactants are dissolved in a solvent within a closed vessel known as autoclave. The vessel is heated under high pressure and above solvent boiling temperature. Basic solvents are desirable as their solubility increases dramatically with an increase in temperature. Good control over size shape and crystallinity can be achieved through this process. The drawbacks of this process are expensive equipment and safety issues during reaction as chances of autoclave explosion if not handled properly[31].

1.5.3.3 Sol Gel:

Sol can be described as colloidal solution made up of particles suspended in liquid phase whereas gel can be defined as solid macromolecule in a solvent. Therefore, it is a process in which a liquid with precursors is converted to gel and with further treatment is converted to its solid oxide material. It is a process in which molecular precursors are converted into oxide network through polycondensation process. The idea behind is to dissolve compounds in a solvent and bring it back to solid in a controlled manner. This process allows mixing in

at atomic scale. Dense powder, thin films, porous structures and fibers can be synthesized through this technique[32].

1.5.3.4 Microwave Assisted Synthesis:

This process is based on the interaction of microwave, ranging from 300 MHz to 300 GHz, and precursor material on dipole interaction and ionic conduction mechanism. Heat is generated by dipole interaction when polar end of molecules oscillates with oscillating electric field, hence generating heat. This process is faster than traditional chemical reactions, has higher yield and less byproducts. It can selectively heat either the solvent or precursor material for the synthesis of nanomaterial[33].

1.5.3.5 Sono-Chemical Synthesis:

In this process acoustic cavitation is caused due to irradiation caused by ultrasonic waves. These generated bubbles in the solvent which grows and implode causing hot areas of high temperature and pressure. It is a method in which we can synthesize nanoparticles with controlled morphologies in less time. The disadvantage of this process is that it is an energy intensive process[34].

1.5.4 *Biological Methods*

Nanoparticles can be synthesized using biotic species like bacteria, protein and plants extract. In this synthesis technique nanoparticle are synthesized using processes like biologically induced Bio-mineralization (BIM) and biologically controlled bio-mineralization (BCM) [35]. In BCM, nanoparticles are synthesized naturally using environmental parameters like temperature, redox potential, partial pressure of oxygen and carbon dioxide and pH. This is an extracellular type of synthesis for nanoparticles. If the synthesis of nanoparticles is done through the process of bacteria reduced by Sulphur, then the process is known as biologically controlled bio-mineralization. The process occurs in absolute geochemical environment as the whole process occurs at a specific site, like within cell wall or cytoplasm, completely separating it from the external environment hence making a much-controlled process giving us a better morphology and size of end nanoparticles. Although biological synthesis of nanoparticles is a green synthesis method, then end particles are not monodispersed and the synthesis process is slow[36]. The summary of advantages and disadvantages of the following synthesis techniques are summarized below in table 2.

Table 2. Summary of pros and cons of nanoparticles' synthesis techniques

| Method | Advantages | Disadvantages |
|----------------------------------|--|---|
| PHYSICAL METHOD | | |
| Gas Phase Deposition | <ul style="list-style-type: none"> Fine powder is produced High purity | Inability to maintain size of nanoparticles throughout the experiment Controlled and expert approach is required |
| Electron Beam Lithography | Produces fine size nanoparticles (<50nm) | <ul style="list-style-type: none"> High production cost Lengthy process Resolution limitations |
| Pulse Laser Ablation | <ul style="list-style-type: none"> Fast, Simple, Cost effective Controlled parameters like pressure, temperature and density | High kinetic energy causes re-scattering causing inhomogeneous energy distribution of laser beam |
| Laser-Induced Pyrolysis | Produce particles less than 10 nanometers | Difficulty in obtaining uniformity Broad size distribution of end particles are obtained |
| Ball Milling | Nanoparticles with good dispersion is obtained <ul style="list-style-type: none"> Nanoparticles can be synthesized on industrial scale | Agglomeration due to fine particles interaction |
| CHEMICAL METHODS | | |

| | | |
|--------------------------------|---|--|
| Co-precipitation | <ul style="list-style-type: none"> • Simple process • Ambient working conditions • Can control particle size | reactants with different precipitation rates are difficult to work with in this process Impurities may also get precipitated during the reaction |
| Hydrothermal | Precise control on size shape, crystallinity and distribution of final product <ul style="list-style-type: none"> • Significantly enhanced chemical reactivity of reactants | Expensive autoclaves required And safe reaction process. |
| Sol Gel | Uniform mixing of precursors at molecular level <ul style="list-style-type: none"> • High purity products • Better control over product final composition • Controlled porosity can be obtained | <ul style="list-style-type: none"> • Longer reaction time • Harmful organic solvents |
| Microwave Assisted | <ul style="list-style-type: none"> • Faster chemical reactions • Higher yields • Lesser side products | Expensive equipment <ul style="list-style-type: none"> • Difficult to scale up • Difficult monitoring of reaction |
| Sono-Chemical Synthesis | Ambient temperature synthesis of nanomaterials High reaction rate and lesser reaction time <ul style="list-style-type: none"> • Simple method | Energy intensive process <ul style="list-style-type: none"> • Difficult to scale up • Technique not for heat sensitive material |
| Biological Methods | <ul style="list-style-type: none"> • Green synthesis process | <ul style="list-style-type: none"> • Lower yield • Slow reaction rates |

1.6 Drug Delivery applications of MNP

Delivery of healing drugs to the specific site of tumor is defined as the Drug delivery. It helps in treating diseases like cancer, heart related viruses and unwanted microbes. Conventional techniques like chemotherapy, radiation and surgery are less effective and may have many undesirable effects due to which we are encountering rising trend in cancer cases in both developed and under- developed countries. The various reasons for their little effectiveness include the fact that chemotherapeutic drugs fail to achieve desired levels at the targeted sites due to immunological responses leading to elimination of that drug through excretory system and inability of the surgical procedures to completely eradicate the cancer

cells from the body. Due to which the drug injected would not be able to reach target site to completely eradicate the tumor. These drugs are also harmful to healthy cells within the body. Whereas drug delivery offers the advantage of target specific delivery with minimal side effects. Magnetic nanoparticles are widely used for this application as these nanoparticles have superior properties like superparamagnetic nature, biocompatible and nontoxic nature[37]. These particles can be guided within the body through external magnetic field. The whole process includes drug loading in which drug is loaded on the nanoparticles and is injected into the body. Then comes targeted delivery, in which with the help of outer magnetic field, drug is transported to the tumor spot and is released through different mechanisms like change in temperature, pH and osmolality. Lastly the nanoparticles are removed from the body with the help of kidney, spleen and liver. The delivery of drug to specific site can also controlled by imaging techniques like MRI[38]. Targeted drug delivery Idea was introduced in 1970's [39]. Drug delivery is further categorized in two forms known as active targeting and passive targeting. Passive targeting is based on the mechanism of increasing drug concentration at the site of tumor by the help of permeation and retention effect and due to the physiochemical properties of nanoparticle which includes size and surface properties. This process offers advantage of high retention of drugs at the tumor site hence increasing the effectiveness of the drug. Despite having advantages this form of targeting has the limitation of poor reliability as it is a less controlled mechanism. Whereas active targeting offers advantage of controlled manner delivery of drug as this process is controlled by external magnetic field which helps guiding the particles to the target site and also improves stabilization of nanoparticles at tumor site[40]. Ligands functionalization of MNPs allows further stabilization and accumulation at the tumor site. When drug loaded nanoparticles enter the body through veins their surface is attached by plasma protein on the hydrophobic points and gets recognized by body immune system and thus excreted out of the body. Therefore, in order to retain these nanoparticles within the body surface functionalization of these nanoparticles can be done by hydrophilic compounds like polyethylene glycol (PEG) to make these nanoparticles more biocompatible and more water soluble. Effective treatment by the help of nanoparticle depend upon various factors including nanoparticles concentration, movement time and blood movement rate, biocompatibility of nanoparticles, external magnetic field strength, size and shape of nanoparticles, magnetic properties of nanoparticles, distance and depth to travel by nanoparticles to tumor site and blood flow rate. The drug loaded magnetic nanoparticles are injected into the veins in the form of colloidal suspension and then delivered to the tumor

site through external magnetic field[41]. Targeted drug delivery offers advantage of efficient use of drugs, proper target identification and only releasing drug to effected sites.

1.7 Research Goal

Iron oxide (Magnetite) and TiO_2 nanoparticles are widely used in the field of biomedical science, with a special focus on drug delivery. However, the combined effect of these materials on drug delivery has not been well investigated or not much data is readily available in research, it has not yet been determined how the addition of TiO_2 to iron oxide affects characteristics like drug loading, drug release, and hemolysis when treated at low temperatures. For the first time, the impact of ciprofloxacin loaded on this doped material will be investigated in the present research.

Synthesis of TiO_2 -integrated iron oxide nanoparticles for administering drugs is the main goal of this work. These structures can greatly increase the curative effect of combined drugs by utilizing the magnetic and biological features of iron oxide nanoparticles. Using an external magnetic field, iron oxide nanoparticles can be actively targeted to tumor locations due to their magnetic traits. These nanoparticles' size and shape affect how effective they are. To ensure steady behavior within the body, a size smaller than 100 nm and a restricted size distribution are ideal for biomedical applications.

1.8 Aim of study

The aims of this study are as follows:

- Successful Synthesis and characterization of $\text{Fe}_3\text{O}_4/\text{TiO}_2$ nano particles through hydrothermal method.
- Evaluation of drug loading and drug release behavior of $\text{Fe}_3\text{O}_4@\text{TiO}_2$ with Wt % (5%, 10%, 15%, 20%).
- Analyzing and evaluating the hemolysis of these synthetic nanoparticles—both bare and drug-loaded (ciprofloxacin).

CHAPTER 2: LITERATURE REVIEW

2.1 Iron Oxide Nanoparticles:

Among various types of nanoparticles Magnetite (Fe_3O_4) and Hematite (Fe_2O_3) because of their amazing qualities, including their superparamagnetic nature, biocompatibility, environmental friendliness, and stability, these are the most extensively utilized nanoparticulate system. Hematite is one of the ancient iron ores that has been utilized by humans as a pigment.

It has been found that natural hematite can be used in antimicrobial activities when used as a cathode material. Since ferrite is superparamagnetic once it is smaller than 100 nanometers, it can be controlled by an external magnetic field.[41]. Dispersion is the main focus for these nanoparticles. Nanoscale particles have a higher surface area to volume ratio due to which aggregation and agglomeration occurs. So, to use for various application surface needs to be modified as size and shape plays important role in how nanoparticulate system performs. So, for modification of surface, surface functionalization is used which helps good dispersion of nanoparticles and also helps to connect with another nanoparticle for advance applications[42].

The iron oxide nanoparticle's fundamental structure has oxygen anions, and iron cations inhabit the tetrahedral and octahedral positions. It is possible to see reflection peaks in the magnetite cubic closed pack structure at (200), (311), (400), (422), (511) and (440). Fe (+3) filled two-third of the crystal structure sites[43, 44]. Hematite is another mineral that exhibits an XRD pattern and a hexagonally packed structure. at (012), (104), (110), (113), (024), (116), (214) and (300)[45].

Magnetic material consists of magnetic dipoles that can retain magnetization due to alignment of dipoles under the effect of external magnetic field. Whereas superparamagnetic iron oxide nanoparticles show magnetic effect only in the presence of external magnetic field showing no hysteresis after the removal of external magnetic field[46]. The property is a plus for biological applications as they become detectable from external magnetic detectors as they produce heat in the presence of magnetic field. Various ores of Iron behave differently in the presence of magnetic field and at different temperatures. Talking about hematite its ferrimagnetic at room temperature and at -10 degree centigrade it changes to antiferromagnetic state. Magnetite at size rang below 20 nm act as super paramagnetic in

nature[47] whereas maghemite becomes unstable at higher temperature and show not effect under external magnetic field and at room temperature it is ferrimagnetic in nature.

The ability of nanoparticles to remain monodispersed and resist agglomeration determines their colloidal stability. Iron oxide nanoparticle usually gets degraded and agglomerated due to collision occurring within the particles in the suspension which depends on three major factors including concentration of particles, hydrodynamic flow and Brownian motion generating attractive and repulsive forces[48]. So, the goal is to create an environment in which repulsive forces are higher than attractive forces within the suspension so that particle don't get agglomerated. In order to increase repulsive forces surface functionalization process is used in which outer surface of nanoparticle are covered by polymers including chitosan, Polyethylene glycol, starch and dextran etc. and other organic materials like silica, ascorbic acid and citric acid plays important role in surface functionalization of iron oxide nanoparticle[49]. These coatings are also reducing toxicity, as most of them are biodegradable. Good stability is indicated by zeta potential value above 25mV or below -25mV[50].

Features of iron oxide nano particles rely on the shape, size and crystallinity of synthesized nanoparticles. These characteristics primarily depend upon the reaction parameters and synthesis process. Iron oxide nanoparticles less than 20 nanometer[51] plays important role in biomedical applications as below this size range nanoparticles can easily enter tumor site crossing all barriers and creating therapeutic outcomes[52]. Round and crystalline nanoparticles are favored, therefore form and crystallinity are also important.[53].

Toxicity of nanoparticles is the main barrier to their biomedical application. They get accumulated within the body and become hard to remove as it is found in previous research that superparamagnetic iron oxide nanoparticles get accumulated within the kidney of rats during experimental trails. So, to reduce the toxicity biocompatible and biodegradable coatings are used. Within Iron ore magnetite nanoparticle are found to be less toxic.

2.2 Surface Modification of Iron Oxide Nanoparticles:

Iron Oxide nanoparticles are hydrophobic in nature[54]. These nanoparticles contain high surface area to volume ratio due to which agglomeration occurs when particles interact which each other forming clusters which acts as ferromagnetic in nature and when these clusters interact with each other results in further magnetization of these nanoparticles[55]. Ferro fluids are the magnetic nanoparticles of iron oxide which exist in a form of colloidal solution which is applicable to various biomedical applications. These magnetic

nanoparticles suffer from aggregations issue which can be overcome by surface coating or surface functionalization[56]. These surface modifications play's important role in preparing nanoparticles for biomedical applications. Surface functionalization also plays an important role in enhancing stability and reducing toxicity of nanoparticles. Surface modification can be done by the process of ligand addition method in which material used for surface functionalization like polymers or surfactants are added with the precursors of nanoparticles which get attached to nanoparticles produced by electrostatic or hydrophobic interactions and prevent agglomeration[57]. Second method of modification surface includes the process of ligand exchange in which the original particles surface is changed by functional groups like amine, carboxylic acids, Thiols, Diols etc. The surface of nanoparticles is functionalized according to specific drug nature and the tissue to be targeted. So, the modification of nanoparticles is done through the process of polymer surface exchange or polymer encapsulation process. In Encapsulation method the surface of particles is exchanged by the polymer and polymer encapsulation occurs through the process of functionalization in the mechanism of polymer encapsulation process. The polymer used for encapsulation or surface exchange could be of various types which could be synthetic in nature like polyvinylpyrrolidone (PVP), polyethylene glycol (PEG), polyvinyl alcohol and poly lactic coglycolic acid etc[58]. These polymers could be natural in nature like chitosan, starch, gelatin or dextran etc. Chitosan in natural polymers is the most widely studied for biomedical applications due to natural abundance and superior properties like biodegradable, nontoxic, biocompatible and its attractive hydrophilic nature. It consist of repeated units of hydroxyl and amino group which make it suitable for therapeutic purposes like gene-delivery[59]. The limitation of chitosan of poor solubility can be solved by its derivatization which makes lit glycol chitosan which becomes soluble in acidic and neutral pH environment due to glycol branches[60].

2.3 Iron Oxide Based Drug Delivery:

Iron Oxide nanoparticles are approved by Food and Drug Administration (FDA) for the use for biomedical (in vivo) applications as its ore magnetite and maghemite naturally exist in human body and are biocompatible in nature. Magnetic Drug Targeting on tumors has a recovery rate of about 57% as most particles localized on tumor surface. It is better than the conventional method as only 1% of the drug can reach the target site showing extremely low targeting efficiency. Superparamagnetic Iron Oxide nanoparticles (SPIONs) have excellent penetration depth of 10 to 15 centimeter as smaller crystallite size allows them sufficient

thermal energy to oscillate in the direction of magnetic field.

Cancer is caused by uncontrolled division of abnormal cells that spread throughout the body damaging organs and healthy tissues. It is one of the leading causes of death all around the world. Chemotherapy, radiations, and surgery are the traditional treatments used to cure this disease which are less effective, noncurative, time limited and lacks specificity having potential to cause severe damages to healthy cells.

The commonly used drugs for the cure of cancer includes Doxorubicin (DOX), Docetaxel (Dtxl), Cisplatin, Bortezomib, Gemcitabine (GEM), Artemisinin and Paclitaxel (PTX). DOX intercalates into the cell DNA and inhibits the DNA replication by inhibiting topoisomerase II[61]. Dtxl inhibits the cell growth by disruption of microtubules dynamics[62]. Cisplatin induces cell damages by crosslinking with the DNA purine bases. Bortezomib inhibit the cell growth by inhibiting protein complexes known as proteasomes which degrade proteins[63]. Gemcitabine impedes DNA long chains which results in cell death. Artemisinin produces free radicals which causes cell damages and slowing the division of tumor cells[64]. PTX disrupts the normal tubule dynamics required for cell division[60].

Magnetic resonance imaging (MRI) assessed targeted drug delivery with the help of iron oxide nanoparticles are extensively studied as they can also be used as a contrast agent with effective drug loading properties. Therefore, Iron Oxide nanoparticles aid in monitoring tumor sites and the treatment against them.

Oleate coated iron oxide nanoparticles synthesized by pyrolysis method of 15 nm size were synthesized by **Xie Et al.**[65] and were studied by labeling them with ^{64}Cu -DOTA and Cy5.5 which shows prolonged circulation and accumulation at tumor site. Further these nanoparticles were encapsulated with doxorubicin along with dopamine in human serum albumin for tumor targeting having hydrodynamic diameter of around 50 nm termed as 'D-HINPS. These encapsulated nanoparticles were studied on murine breast cancer model in which it was proved that these nanoparticles have higher tumor clampdown and higher accumulation effect with respect to doxorubicin and doxil alone. In another in-vitro study these nanoparticles showed better drug loading capabilities due to polyamine coating promoting better cellular uptake[66].

Folic acid conjugated iron oxide nanoparticles were synthesized for the treatment and diagnosis of breast cancer by **Huang Et al.**[66]. The efficacy of these nanoparticles was tested by loading them with Dox and were tested on nude mice having MCF breast cancer

tumor. The accumulation of these nanoparticles was tested using MRI as iron oxide nanoparticle have higher R2 reflexivity[67]. Iron oxide nanoparticles coated with heparin loaded with Dox was studied for combined drug delivery and MRI applications. The synthesized system showed better drug uptake efficiency, less cardiotoxic effect and slower drug release rate with respect to Dox alone[68].

There is great potential for therapeutic applications such as drug administration using magnetically guided iron oxide nanoparticles in the biomedical field. The tumor location is reached by means of an external magnetic field, which additionally promotes the aggregation of these nanoparticles there. [69]. The importance of these nanoparticles' saturation magnetization is crucial in these applications whilst a higher saturation magnetization would provide more control over the particles' trajectory.

Iron oxide nanoparticles were synthesized via coprecipitation method by **Wagstaff Et al.** [69] group. These nanoparticles were coated with using the process of “iterative hydroxylamine seeding” method. With the Help of polyethylene glycol linker, the cisplatin was loaded on these nanoparticles. The synthesized nanoparticles displayed a 110-fold rise in cytotoxicity on cancer cell line of human ovarian and inhibition of cell growth when attracted by bare magnet.

Iron Oxide nanoparticles were synthesized by **Unterweger Et al.**[70]. These nanoparticles were coated hyaluronic acid which allowed improved drug loading of cisplatin and also enhanced targeting of CD44 receptors in cancerous cells. Formation of polymer metal complex with hyaluronic acid, loading of cisplatin was achieved. The encapsulation efficiency of these drugs was calculated to be around 43.2%. The drug release mechanism was highlighted as burst release on first 30 minutes and after that continuous release for 48 hours indicated as surface bonded drug. An increased drug release was observed which made these nanoparticulate systems suitable for target drug delivery applications. The path of these nanoparticles was controlled by neodymium magnet.

Iron oxide nanoparticles covered with Poly Vinyl Alcohol (PVA) and filled with Dox was studied by **Nadeem Et al.**[71]. Magnetic properties were studied. The control of the path of these nanocarriers was studied through external magnetic field. These nanoparticles showed good control for guided delivery applications of drugs.

Zaloga Et al.,[72] synthesized iron oxide nanoparticles coated with human serum albumin (HSA) and lauric acid, having mean diameter of about 7 nanometer and having mitoxantrone

adsorbed on the surface of HSA, exhibit improved stability and a linear drug release pattern for approximately 72 hours. These synthesized nanoparticulate systems showed potential for site specific targeting in in-vitro systems.

Chitosan coated iron oxide nanoparticles were synthesized by **Natesan and co-workers**. [73] In this study artemisinin was used as an anticancer drug. Chitosan provides added advantage of excellent encapsulation of drugs. Iron oxide nanoparticles with size around 10 nanometers were synthesized by Natesan et al. The drug (chitosan and artemisinin) was loaded on the sample by ion gelation method. Both in-vitro and in-vivo magnetic assisted targeting was examined in glass containers and in mice models. The results showed higher drug accumulation in tumor.

Iron oxide nanoparticle coated with polymerized β -cyclodextrin was studied by **Jeon Et al.** [74]. These nanoparticles were loaded with polymerized paclitaxel by inter-particles interactions. High magnetic saturation was observed showing enhanced anticancer activities.

Therapeutic specificity of a drug is determined by interactions between antigens and antibodies which allows them to specifically target the disease site. Iron oxide nanoparticles are functionalized with targeting agents like peptides or antibodies which aids in site specific delivery of therapeutic agents. Vectorized nanoparticles are the major focus of many research groups and their testing as targeting agent has been an ongoing pursuit.

Iron oxide nanoparticles loaded with gemcitabine (GEM) and further modified with amino-terminal fragment (ATF) peptides were synthesized by **Lee Et al.** [75]. The system was tested on pancreatic cancer tissues which showed increased drug uptake on tumor sites. Peptide linkers used due to enzyme sensitive properties helped in controlled drug release by making cleavages through enzymes in cancer cell's intracellular components. Therapeutic and diagnostic application of this system was observed using MRI technique.

Peptide and carboxymethylated- β -cyclodextrin loaded iron oxide nanoparticles were synthesized by **Mu Et al.** [76]. Nanoparticles with size range of about 30 nanometers were used in this nanoparticulate system and were tested on breast cancer cells. The drug used for this study was paclitaxel and the system along with this drug was tested under in-vitro conditions which showed their abilities to target cancer cells.

Two peptides luteinizing hormone-releasing hormone receptor (LHRHR) and Urokinase-type plasminogen activator receptor (uPAR) were conjugated on iron oxide nanoparticles by **Ahmed Et al.** [77]. These nanoparticulate systems were termed as 'double-receptor-targeting

nanocarriers'. These nanoparticles were tested for treatment and diagnosis of prostate cancer. Both peptides were attached to nanoparticles by formation of amide bonds. These nanoparticles demonstrated good properties like high drug loading, smaller hydrodynamic diameter, and negative zeta potential value. These nanoparticles, loaded with paclitaxel, showed an increase in cancer cell cytotoxicity and reduction in amount of drug needed to have desired results with respect to concentration needed for free drug only. Other vectorizing agents includes aptamers and antibodies that are being used for drug delivery application.

Iron oxide nanoparticles with average inorganic diameter of about 8 nanometers were synthesized by **Nagesh Et al.** [78]. These nanoparticles were coated with β -cyclodextrin (drug incorporated in its hydrophobic cavity) and pluronic F127 polymer. Docetaxel was loaded on these nanoparticles which showed higher penetration into pancreatic cancer cells due to its desired smaller size. The results showed that this nanoparticulate system is preferable for targeting prostate cancer.

To target prostate cancer cells, nanocarriers targeting prostate specific membrane antigen (PSMA) were developed by **Leach Et al.** [79]. In this research nanoparticle were coupled with biotin-streptavidin for nanoparticles functionalization and loading it with Dox. Dox was loaded by intercalating into double helix of aptamer which can identify extracellular areas of PSMA. This system allowed reduction in nonspecific uptake hence reduced untargeted toxicity.

Iron oxide nanoparticles coated with gemcitabine and anti CD44 antibodies were synthesized by **Aires Et al.**[80]. These coatings are capable of targeting CD44-positive pancreatic cancer cells and induce cell death. Iron oxide nanoparticles were functionalized using di-sulfide bonds helping in releasing drug under high reducing environment. The nanoparticulate system showed selectivity towards cancer cells and fast release under reducing conditions.

Use of functional groups or stimuli-sensitive coating allows controlled drug release at specific sites. Variation of pH between healthy and cancerous cells can be exploited for targeting applications. Cancers cells have lower extracellular pH with respect to healthier surrounding cells[81]. So, this pH difference can be exploited using coating, bonding of nanoparticles sensitive to pH such as liposomes or polymers. Using temperature sensitive coating on iron oxide nanoparticles can play an important role in hyperthermia applications

and controlled drug release. Iron oxide nanoparticles with acidic environment sensitive functional groups have been worked on by researchers in the past decade.

Iron oxide nanoparticles were coated by polyethylene glycol (amine terminated) and then loaded with Dox by covalent bonding via hydrazine linkages sensitive to pH by **Kievit Et al.**[82]. This nanoparticulate system is synthesized to overcome drug resistance encountered in drug-resistant cancers. The synthesized nanoparticle had hydrodynamic diameter below 100 nanometers and negative zeta potential value favoring penetration of drugs into the tumor site. The system showed better drug release in acidic environment. This nanoparticulate system was efficient against multi drug resistance (MDR) with respect to free drug alone, hence showing enhanced therapeutic effect.

pH-dependent drug release of nanoparticulated system based on iron oxide nanoparticles was studied by **Gautier Et al.**[83]. In these Dox loaded iron oxide nanoparticle formation of Dox-Fe⁺² complex was evaluated which binds to hydroxyl groups and dissociates in acidic environment. The system was tested at pH value 4, showing potential toward therapeutic applications as drug release rate was substantially increased. Chitosan, biocompatible in nature, having antitumor properties, shows enhanced solubility in dilute acidic environment which makes its attractive for pH dependent drug delivery application[84].

Magnetic nanoparticles coated with chitosan were studied for pH-responsive therapeutic applications by **Unsoy Et al.**[85]. Having core size of about 6 nanometers, iron oxide nanoparticles were synthesized by coprecipitation method and were coated with chitosan by ionic crosslinking of tripolyphosphate (TTP). The system showed high drug release at pH value 4.2. Same results were observed in another study in which iron oxide nanoparticles were coated by chitosan[86]. Increase in cytotoxicity of these nanoparticles was observed that free drug alone. More accumulation of nanoparticles was observed around the nucleus than free drug alone.

Iron oxide nanoparticles with chitosan coating and glutaraldehyde linker that is sensitive to pH for drug delivery of doxorubicin was reported by **Adimoolam Et al.**[87] Due to formation of amide bonds the system became pH sensitive at lower pH values (acidic conditions). The system was found to be effective for delivery of doxorubicin for human breast cancer and ovarian cancer cell lines. Nanoparticles with temperature sensitive coatings of polymers show enhanced drug release under alternating magnetic field.

Chitosan coated iron oxide nanoparticles, mesoporous in nature and loaded with

doxorubicin, was developed by **Zou Et al.**[88]. The system showed enhanced therapeutic effect under alternating magnetic field.

In another study carried out by **Quinto Et al.**, iron oxide nanoparticles were coated with phospholipid-polyethylene glycol having core size of 14 nanometers[88]. The system showed generation of sufficient heat and release of doxorubicin in a controlled manner. Hence proving its application in combined drug delivery and hyperthermia application.

2.4 TiO₂ Applications in Biomedicine:

TiO₂ nanoparticles are often used in PDT to treat cancer as photosensitizers. Reactive oxygen species (ROS), which are produced when TiO₂ is exposed to light, have the potential to cause cancer cells to die. TiO₂ has this property, which makes it useful in antimicrobial treatments even against germs that are resistant to antibiotics. TiO₂ shows enhanced antibacterial activities when combined with ZnO. To make TiO₂ activated by visible light, recent developments have concentrated on doping it with other elements (such nitrogen or silver)[89]. Studies have indicated that doped TiO₂ nanoparticles maintain their antibacterial efficacy in the presence of visible light, expanding their range of applications. In addition, TiO₂ nanoparticles are being researched for applications in medical imaging and biosensors. They are useful for imaging at the cellular level and for detecting biological changes due to their large surface area and capacity to bind different biomolecules[90]. This can support early disease detection and tracking. Due to its biocompatibility and capacity to promote cell proliferation and differentiation, TiO₂ is utilized in scaffolds for tissue engineering. In bone tissue engineering, where TiO₂ increases osteoblast activity and bone regeneration, this is especially pertinent. The unique features of TiO₂ nanostructures, such as non-toxicity, biocompatibility, and affordability, have drawn more interest in the field of medicine. These attributes include NPs, NTs, and nanorods, as well as their composites. The four primary categories of biomedical applications for these intriguing nanomaterials include biosensing, drug transport, antibacterial activity, and implant uses. In recent years, there has been a lot of research done on the possible use of TiO₂ in PEC and electrochemical biosensors for the detection of distinct analytes[91]. The process of electrochemical anodization, which produces TiO₂ nanostructures such as nanotubes (NTs) through nanoscale surface modification of titanium or titanium-based alloys, has garnered much attention and understanding for use in biological applications. For dental or orthopedic implants, it has been demonstrated that anodic TiO₂ NTs and nanostructures with surface modifications that deliver targeted drugs are clinically beneficial approaches for successful

osseointegration and superior osteoinduction, particularly in patients with chronic inflammation, osteoporosis, and metabolic diseases in the future. For the factors like cell adhesion and proliferation, physicochemical qualities, and biocompatibility, TiO₂ nanotubes (TNTs) surfaces have been applied as a coating on metallic biomedical implants, showing encouraging findings in preliminary analyses in terms of integration to living tissues. They also could integrate drugs and regulate their release to the surrounding tissues[92].

2.5 TiO₂ Applications in the Field of Drug Delivery:

By modifying TiO₂ with PEI and FA, a novel kind of multifunctional material known as FA-PEI-MTNP was produced to investigate the viability of mesoporous TiO₂ for targeted drug delivery and light-controlled drug release. Employing TNTs is a viable way to develop different kinds of localized drug delivery systems that can get around the drawbacks of systemic drug therapy. Based on the exceptional qualities of TNTs, such as their high biocompatibility and mechanical and thermal stability, TNT layers can be used as orthopedic and stent implants in any shape or form. This promotes bone cell adhesion, differentiation and proliferation, hydroxyapatite formation, osseointegration, and hemocompatibility [93, 94]. To produce TiO₂ NPs that would be ideal for therapeutic applications, a variety of factors were examined, including molarity, pH, calcination temperature, and synthesis method. TiO₂ with nanotubes has recently advanced, and these advances offer advantageous properties for drug delivery applications. These properties include high surface area, high and versatile drug-loading capacity for multiple drugs, controllable nanotube dimensions, tunable geometries and surface chemistry, and the ability to modulate drug release kinetics[95, 96]. The hydrothermal process can be used to create porous TiO₂ with a pompon-like sphere morphology. The resultant material has several good physical features, such as a large pore volume, high specific surface area, and a pompon-like sphere morphology [97]. TiO₂ spheres' excellent drug sustained-release qualities are demonstrated by the DOX-released test, which displays the drug-release property of the material. A study shows if insulin is injected into Mt and then TiO₂ is added to the composite as a porous inorganic coating, this could delay the breakdown of insulin in the digestive system and lengthen the period that the drug travels through its matrix and enters the target medium [96]. The in vitro drug release results show excellent potential, and the samples continue to release the drug even after 22 hours. Furthermore, by extending the hormone's shelf life, this kind of encapsulation can warn against injecting insulin and instead recommend oral administration, which offers

diabetics a more comfortable and painless course of therapy[98].

Table 3. TiO₂ applications summary in biomedical field

| Application | Description | References |
|--|---|-------------------|
| Drug carriers for the Infusion of Drugs | Drugs can be more stabilized, bioavailable and delivered to specific areas when they are enclosed in TiO ₂ nanoparticles. | [99] |
| Photocatalytic drug release | Exploiting use of the photocatalytic qualities of TiO ₂ to manage the release of medications in both space and time when they are exposed to light. | [100] |
| Antibacterial Coatings | TiO ₂ nanotubes are used to transfer antibacterial compounds to implant surfaces, lowering the risk of infection. | [101] |
| Bone Regeneration | Orthopaedic implants employ TiO ₂ nanotubes loaded with growth hormones and antibiotics to improve bone integration and prevent infections. | [102] |
| Gene Delivery | In the goal to aid gene therapy applications, TiO ₂ nanoparticles are being investigated for their ability to transfer genetic material to cells. | [103] |
| Stimuli-responsive Systems | TiO ₂ based drug delivery systems that release drugs at specific locations in response to external stimuli that involve temperature, or magnetic fields. | [104] |

CHAPTER 3: MATERIALS & METHODS

3.1 Synthesis technique for nanomaterials:

Two different techniques are used to manufacture nanoparticles. The first approach is known as the top-down strategy, and the second is known as the bottom-up strategy. The former is concerned with shrinking the size of existing technological gadgets, whereas the latter builds even more intricate molecular devices on an atomic arrangement. While the top-down technique is useful for integrating macroscopic devices and producing technical structures with a long reach, the bottom-up approach is more suited for producing and organizing short-range order at the nanoscale level. It is anticipated that the optimal equipment integration for nano-based production will result from combining the two methodologies.

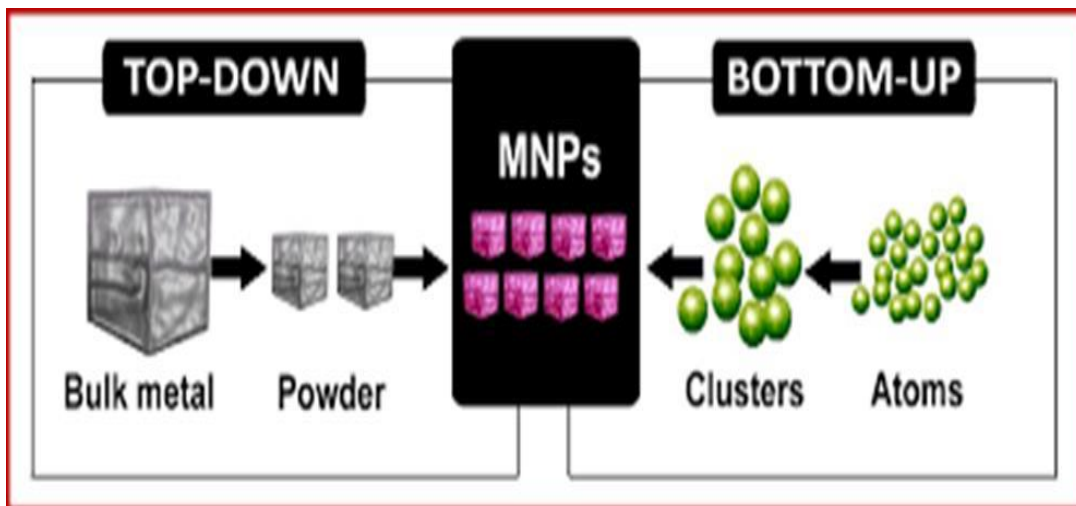


Figure 3.1: Schematics of top-down and bottom-up approach

3.1.1 Top-down approach

In nanotechnology, the top-down method entails reducing bigger structures to the nanoscale. Significant benefits are provided by the top-down method in nanotechnology in terms of:

- Accuracy
- Integration with current technologies,
- Material variety,

- Application diversification,
- Defect control, and
- Time efficiency.

These techniques include:

- Sputtering,
- Ball milling,
- Etching, and
- Lithographic processes.

3.1.2 Bottom-Up approach

The bottom-up approach is used to create nanostructures atom by atom or molecule by molecule.

In nanotechnology, the bottom-up approach has many benefits, including:

- The ability to create a wide variety of materials,
- Atomic-level precision, novel material properties,
- Cost-effectiveness,
- Biocompatibility, and
- Environmental sustainability.

These advantages make it an effective and adaptable technique for advancing the area of nanotechnology and creating cutting-edge applications in a range of industries.

In the field of nanotechnology, the bottom-up approach refers to a set of techniques that start with individual atoms or molecules and develop nanostructures from them. These techniques use physical, chemical, and biological mechanisms to assemble components precisely. The techniques include sol gel method, micro emulsion method, coprecipitation method, hydrothermal method, solvothermal method etc.

3.1.2.1 Sol gel method

The hydrolysis of the precursor in acidic or basic media and the polycondensation of the hydrolyzed products are the two primary reactions in the sol–gel process.

Modifying the surface of substrates is seen to be an efficient use of the sol-gel process. The main benefit of using the sol–gel process is that stable surfaces and a large surface area may be achieved. [105]

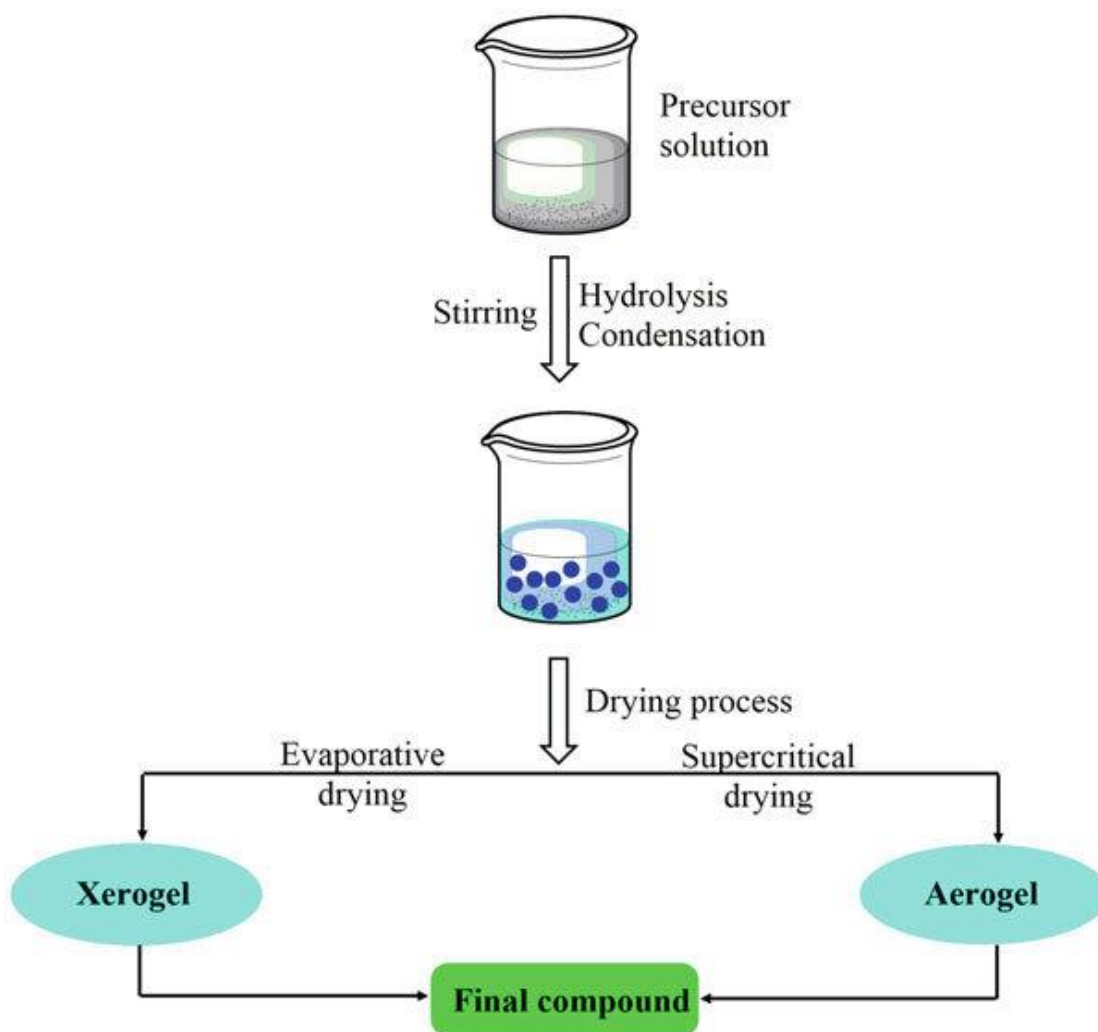


Figure 3.2: Schematic of sol-gel process

3.1.2.2 Coprecipitation Method

Coprecipitation is the process by which multiple compounds precipitate out of a solution at the same time. It is the most practical and affordable method for preparing NPs. This process involves the precipitation of metal in the form of hydroxide from a salt precursor in a solvent with the presence of a base. To precipitate hydroxide, the cation and anion solutions are combined while being constantly stirred, and the resulting oxide is then dried. Coprecipitation involves several simultaneous processes, including initial nucleation, growth, coarsening, agglomeration, and ripening. The synthesis of monodispersed NPs is facilitated by the regulated release of anions and cations, which controls the kinetics of nucleation and particle development [106].

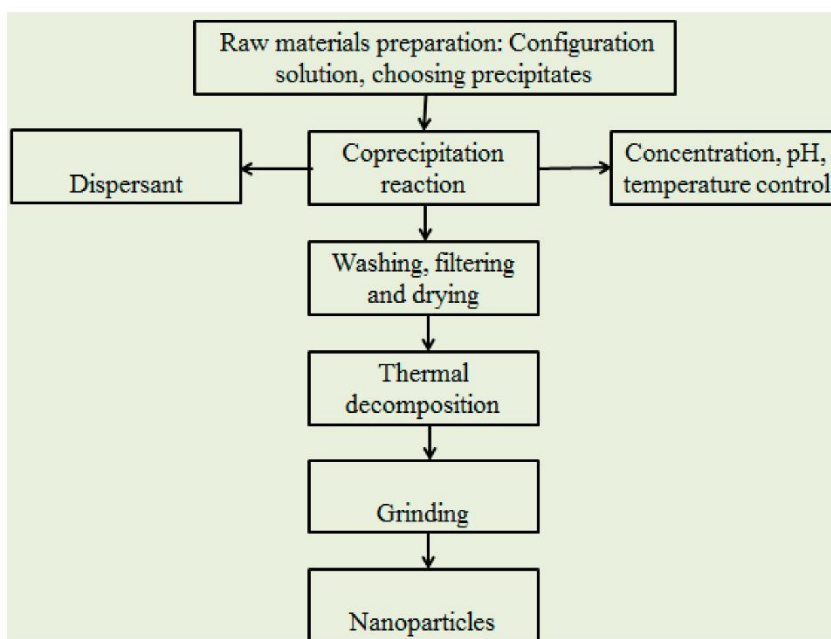


Figure 3.3: Flow chart of coprecipitation method

3.1.2.3 Hydrothermal Method

The process of creating single crystals via hydrothermal synthesis relies on the solubility of minerals in hot water under high pressure. The crystal development process is carried out in a device that consists of an autoclave, a steel pressure vessel that holds water and nutrients [107].

The circumstances of the reaction are crucial during the hydrothermal reaction process. Temperature, time, and kind of solvent all influence how the products are synthesized [108].

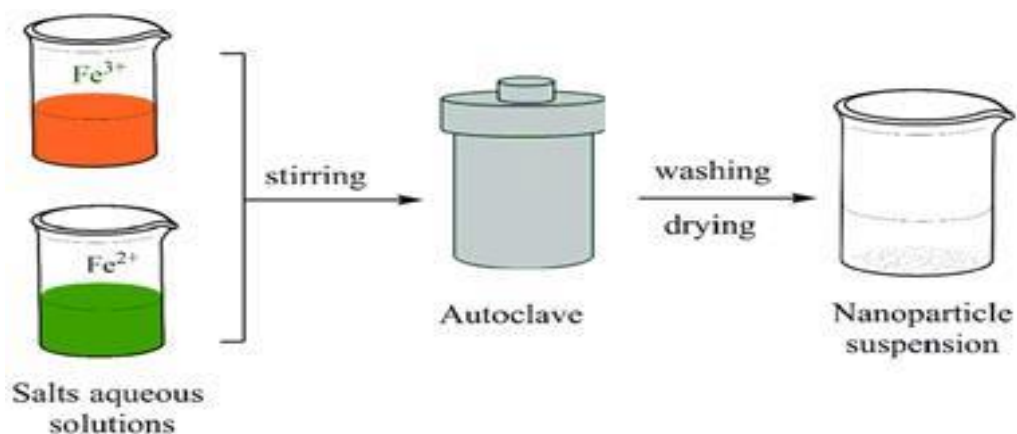


Figure 3.4: Hydrothermal process

3.1.2.4 Microemulsion Method

One of the latest and most effective approaches for creating inorganic nanoparticles is the micro-emulsion approach.

When an inadequate amount of an appropriate surfactant is mechanically dispersed with the oil and water, it forms an emulsion. This two-phase dispersion contains one phase consisting of surfactant-coated droplets that are scattered throughout the continuous other phase.

The intermuscular exchange rate sometimes controls the total reaction rate in situations where reaction rates are extremely fast.

A distinct oil and water system will be created if a surfactant with balanced hydrophilic and lipophilic characteristics is employed at a suitable concentration. Although the system still functions as an emulsion, it has several traits that set it aside from the previous discussion of milky emulsions. They call these new systems "microemulsions." A comparison of emulsions

with microemulsions reveals differences in droplet sizes, visual appearance, energy required for creation, and the interfacial tension between phases.

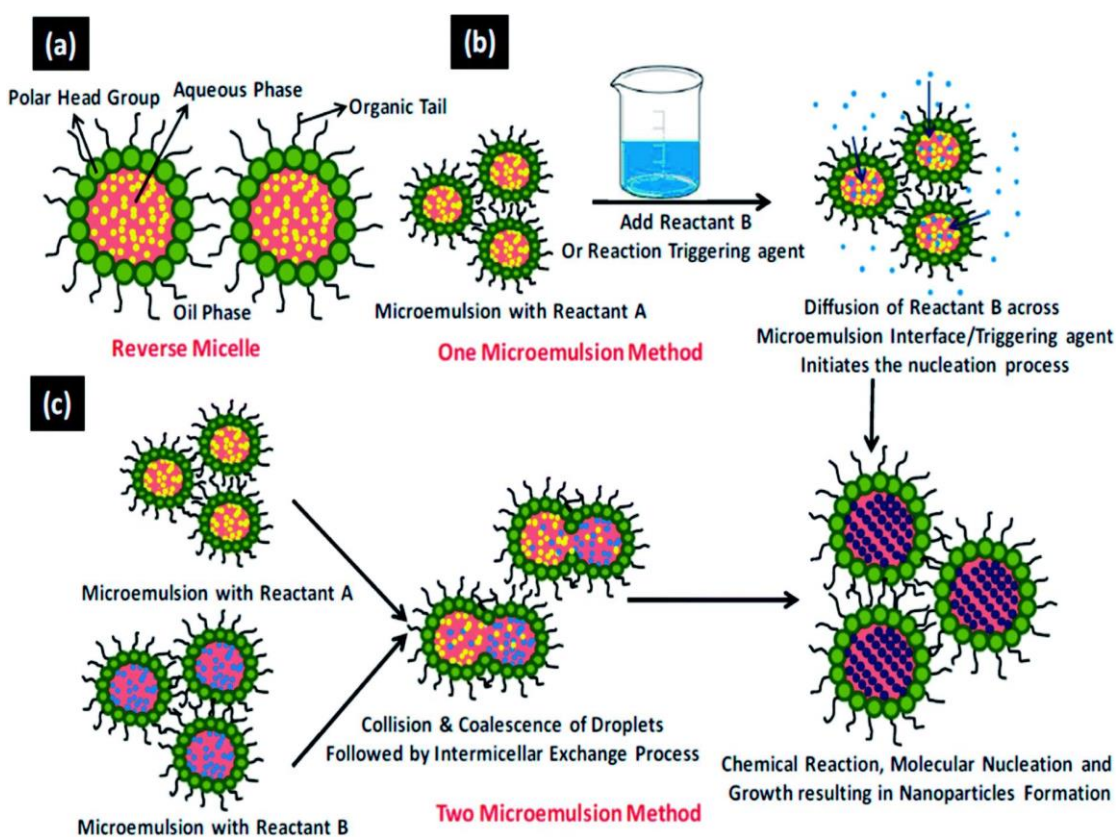


Figure 3.5: Micro emulsion process

3.2 Synthesis of Fe₃O₄@TiO₂:

The synthesis route chosen for making nanoparticles was hydrothermal technique. Hydrothermal method is useful for both industrial and research applications in a variety of areas since it provides a flexible and efficient means of synthesizing nanoparticles with specific features. It is possible to accurately influence hydrothermal conditions, such as temperature, pressure, and reaction time, to impact the nucleation and development of nanoparticles. This makes it possible to create nanoparticles with a regulated morphology and a homogeneous size distribution, including spherical, rod-shaped, or nanoplatelet-shaped particles. High purity and homogeneity nanoparticles are produced by the hydrothermal technique, which is essential for numerous applications in the biomedical, electronics, and catalysis domains.

3.2.1 *Materials:*

Ferric chloride hexahydrate (FeCl₃.6H₂O (99% pure)) was purchased from Merck, ferrous chloride tetrahydrate (FeCl₂.4H₂O (99% pure)) was purchased from sigma Aldrich, reducing agent Ammonia Solution (32%) was used, Ciprofloxacin was used as a sample drug and Deionized water was used for preparation of all solutions.

3.2.1.1 *Synthesis of Fe₃O₄:*

In deionized water, 0.2 moles of FeCl₃.6H₂O and 0.1 mole of FeCl₂.4H₂O were mixed and dissolved to produce magnetite nanoparticles. At 45°C and 800 rpm, the mixture was stirred together. After 30 minutes of stirring Ammonia (32%), was added rapidly until the pH reached 11. After agitating the mixture for half an hour, the 100 ml Teflon-lined autoclave was heated to 120°C for 4 hours. Autoclave was cooled at room temperature and nanoparticles were magnetically separated and repeatedly cleaned with ethanol and deionized water. The particles were then dried overnight. The final product was further grinded to obtain fine powder.



Figure 3.6: Hydrothermal synthesis process of Fe_3O_4

3.2.2 Synthesis of TiO_2 :

Commercial TiO_2 powder was employed for manufacturing TiO_2 nanoparticles. A hydrothermal approach has been selected for generating TiO_2 nanoparticles. A mixture of 5 g of TiO_2 powder and 60 ml of DI water was mixed and stirred at 800 rpm for 1 hour. After 15 minutes of sonication, the mixture was autoclaved at 75 degrees for 4 hours. Solution was allowed to cool to room temperature before being repeatedly cleaned with ethanol and DI water until the Ph reach 7, the solution was dried at 60 degrees overnight, and the resulting powder was calcined at 500 degrees for 4 hours.

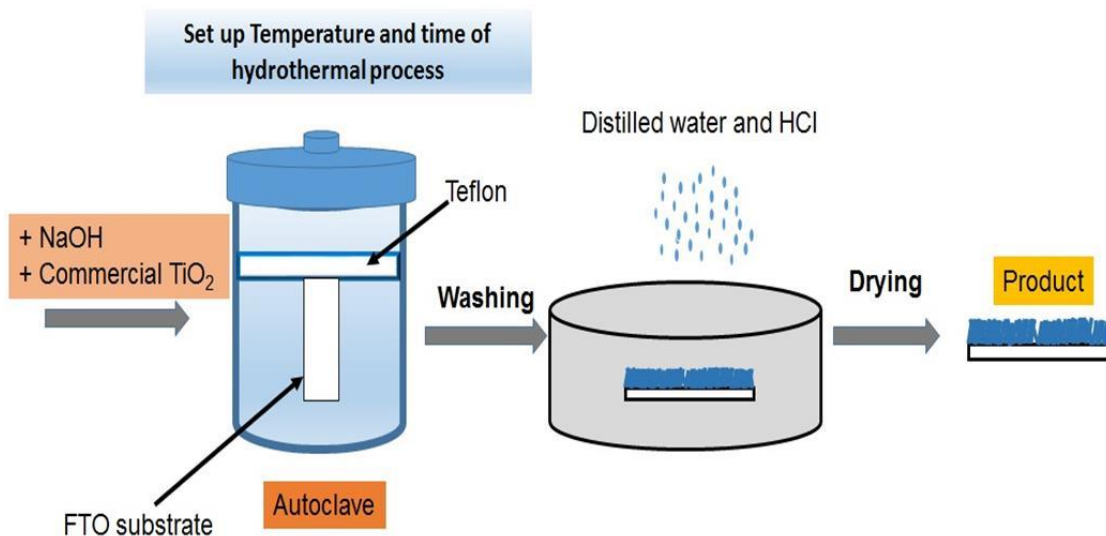


Figure 3.7: Hydrothermal synthesis of TiO₂

3.2.3 Synthesis of Fe₃O₄@TiO₂ nanoparticles:

To produce Fe₃O₄/TiO₂ nanoparticles, Fe₃O₄ was chosen as the core material and TiO₂ was added at weight proportions of 5%, 10%, 15%, and 20%. The two powders were manually ground and mixed for 2 hours. The combination was subjected to 40 minutes of sonication after the ground material had been dissolved in DI water. Afterwards, the particles were once again dried over night at 80° and crushed for an hour to obtain fine powder of Fe₃O₄@TiO₂.

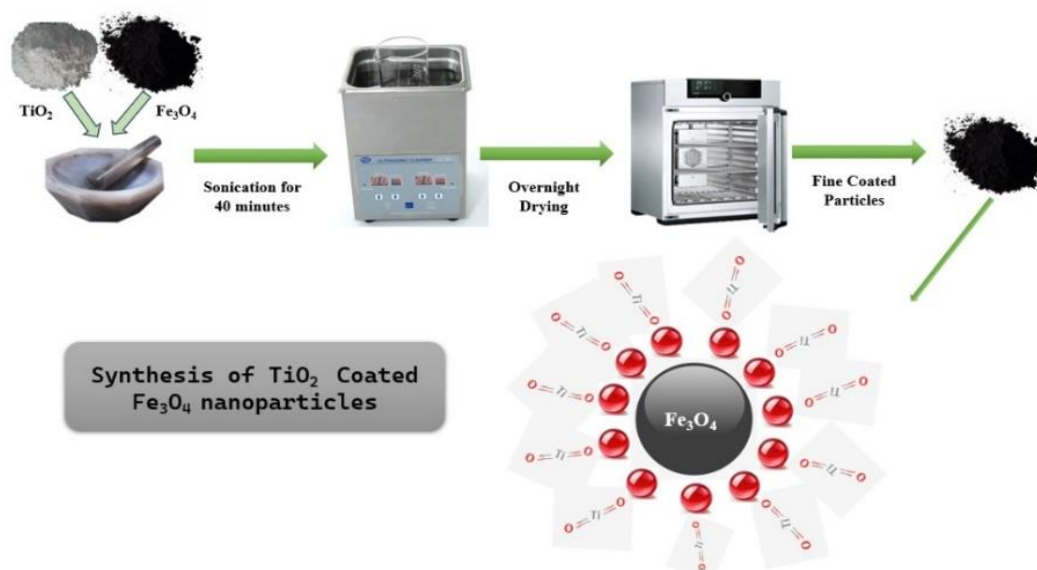


Figure 3.8: Synthesis of TiO₂ coated Fe₃O₄ nano particles

3.3 Drug Loading on Nanoparticles:

To load the synthesized nanoparticles, ciprofloxacin was employed as a sample drug. For each composition (5%, 10%, 15% ,20%) 15 mg of ciprofloxacin was dissolved in 10 ml ethanol to bring the drug concentration to 1.5 mg per ml (1.5 mg/ml). To load the drug all compositions with drug were stirred for 24 hrs. After that, the drug-loaded material was separated using a centrifugation method that took 15 minutes at 12000 rpm. The amount of unloaded drug was determined by analyzing the residual supernatant using a UV-vis spectrophotometer absorption spectrum at 264 nanometers.

3.4 Drug Release Study:

UV Vis spectroscopy was used to measure the drug release percentage after drug-loaded samples were dissolved in 30 ml of buffer solution and continuously stirred at 37 °. The drug release investigation lasted for 24 hours. At certain intervals, 3 ml of PBS solution was taken out of the mixture and replaced with fresh PBS to keep the solution's volume constant.

3.5 Hemolysis Assay:

The hemolysis assay was performed on freshly drawn human blood. After collecting 5 µl of blood, it was centrifuged for 5 minutes at 4000 rpm. At least three times the procedure was carried out. Following the removal of blood plasma, RCBs were cleaned using a PBS solution. A 0.47:9.53 ratio was used to prepare the PBS and RCBs solution. In the Eppendorf tubes, 20 µl of nanocomposites and drug-loaded nanocomposite and 180 µl of blood suspension were combined, and the mixture was incubated for one hour at 37°. Samples were centrifuged once more for 10 minutes at 1200 rpm following incubation. Eventually, supernatant solutions were transferred to 96-well plates along with PBS solution, and the absorbance was measured at 530 nm using a UV -vis-spectroscopy.

3.6 UV -Vis Spectroscopy

UV-Vis analysis was carried out between the range of 200 – 550 nm to evaluate the absorbance of Fe₃O₄ and Fe₃O₄/TiO₂ for drug delivery applications. Samples were prepared by dissolving 5mg of nanoparticles in 5 ml of DI water, Quartz cuvettes were utilized to analyze the solution.

CHAPTER 4: CHARACTERIZATION TECHNIQUES

4.1 X-Ray Diffraction Technique:

A nondestructive technique used to find out the lattice spacing of crystalline solids which can be used to identify elastic properties residual stresses and identification of unknown material. Lattice spacing is determined when x rays enter the material with known wavelength and angle which passes through atomic planes and gets refracted to diffractometer through which the intensity is measured. X-rays are fired toward the sample at different angles so that planes at different angles can be activated so that proper identification of planes present can be identified. Miller indices (hkl) and atomic spacing of powder sample are usually identified by irradiation of these powders through X-rays. The intensity readings obtained correspond to a specific element or phase. Multiple intensity peaks can be seen in the sample containing multiple elements or phases present.

X-rays are generated by a copper target material when electrons produced from a heated filament bombard the target material which dislodges the inner shell electrons. These produced x-rays are collimated and directed onto the sample from where these X-rays deflects back by satisfying brags law through constructive interference and gets recorded by a diffractometer which converts these signals to counts (peaks) recorded on computer screen.

X-Ray Diffraction is used for identification of crystalline phases present and their respective orientation. It is also used for determination of structural properties like grain size, strain, lattice parameters, atomic arrangement, composition of phase present and measuring thickness of thin films and multi layers material.

To analyze the nanoparticles through XRD for structure and phase identification, a small quantity finely grinded nano powder is taken and was tested through XRD machine available at angle 2θ , scanning from 0° to 75° at step size 0.04 for 50 minutes. The obtained results were compared with reference JCPD file for phase identification. For calculation of crystallite size, Scherrer equation is used.

$$\text{Crystallite size}(nm) = \frac{\text{shape factor}(k) \times \text{XrayWavelength}(\lambda(nm))}{\text{Cos}(\theta(\text{radians})) \times \text{FWHM}(\text{radians})}$$

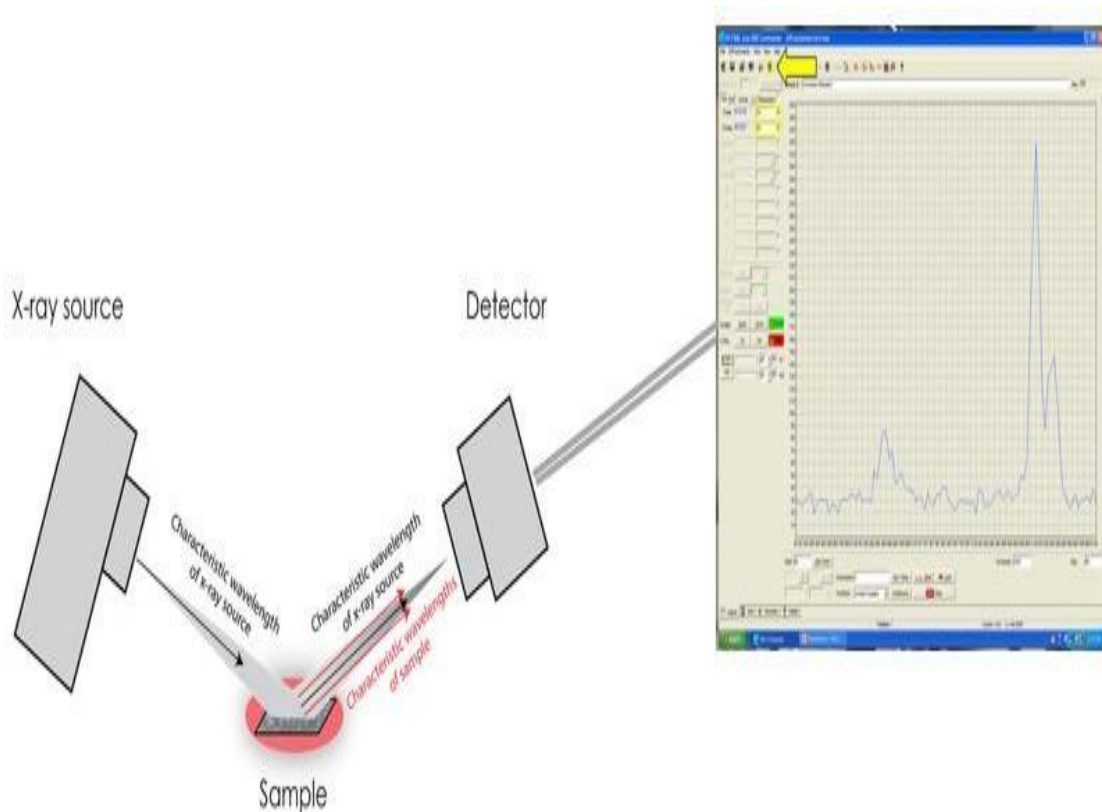


Figure 4.1:Experimental setup of XRD technique

4.1.1 Working Principle of XRD

The powdered form sample is placed under X-ray beam for analysis and rays reflected from plane of crystal material. The interference only takes place when incidence angle is exactly same as reflection angle. Bragg's law is defined by:

$$2d\sin\theta = n\lambda$$

According to Bragg's law, the incident ray is only reflective when there is a $2d\sin\theta$ path adaptation between two sets of planes. The distance between each set of planes is equal to d . The following prerequisite must be met for constructive practical interference:

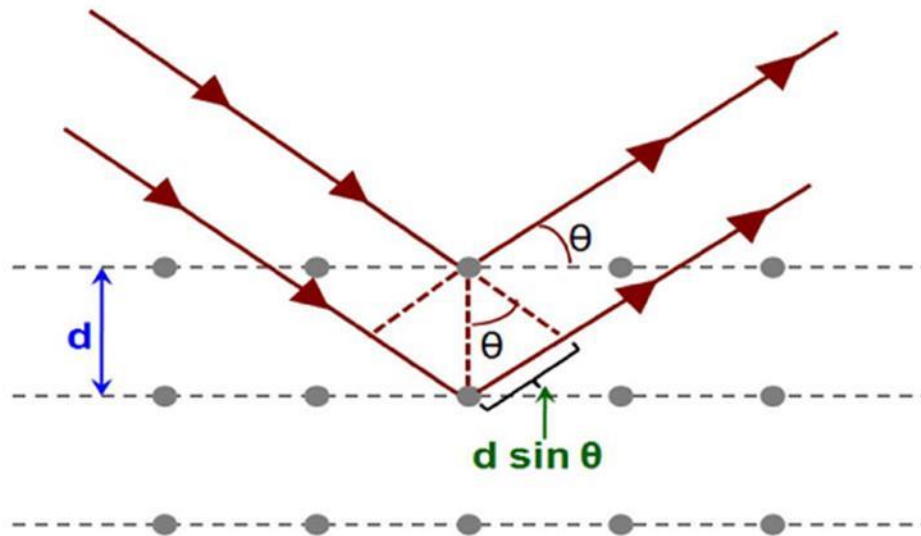


Figure 4.2: Incident x-ray beam scattered by atomic plane in a crystal

4.1.2 Crystal Structure

Generally, three techniques are applied to evaluate the crystal structure of synthesized material.

- **Laue Method**
- **Rotating Crystal Method**
- **Powder Method**

4.1.2.1 Laue Method

Using white light in a reflected or transmitted geometry, the Laue method assists in detecting the orientation of single crystals.

The primary applications of the Laue method, an X-ray diffraction technique, are the internal structure of materials and the crystallographic orientation of single crystals. Through this method, a stationary crystal is subjected to a broad spectrum (white beam) of X-ray radiation.

The Laue method uses a polychromatic X-ray beam, which has a range of wavelengths. Various wavelengths of the white beam simultaneously satisfy the Bragg condition for specific pairs of lattice planes when they interact with the crystal. The spots that correspond to the different lattice planes that diffract the X-rays contribute to the final diffraction pattern. A photographic film or a digital detector positioned behind the crystal can capture the Laue pattern created by these spots.

4.1.2.2 Rotating Crystal Method

A single crystal is anchored on one axis, cylinder-shaped film is wrapped around it, and the crystal is spun in the chosen direction.

4.1.2.3 The Powder Method

A popular method for determining the phase composition, crystallographic structure, and other characteristics of crystalline materials is the powder crystal method, sometimes referred to as powder X-ray diffraction (XRD). Polycrystalline samples or materials that are available in powdered form are especially well suited for this approach.

Crystals in a powder sample have random orientations. All possible crystallographic planes are thus open to diffraction when X-rays are focused on the sample.

Bragg's Law is the core principle of powder XRD

$$n\lambda = 2d\sin\theta$$

The concentric rings or peaks that result from the diffracted X-rays are indicative of the various lattice plane sets.

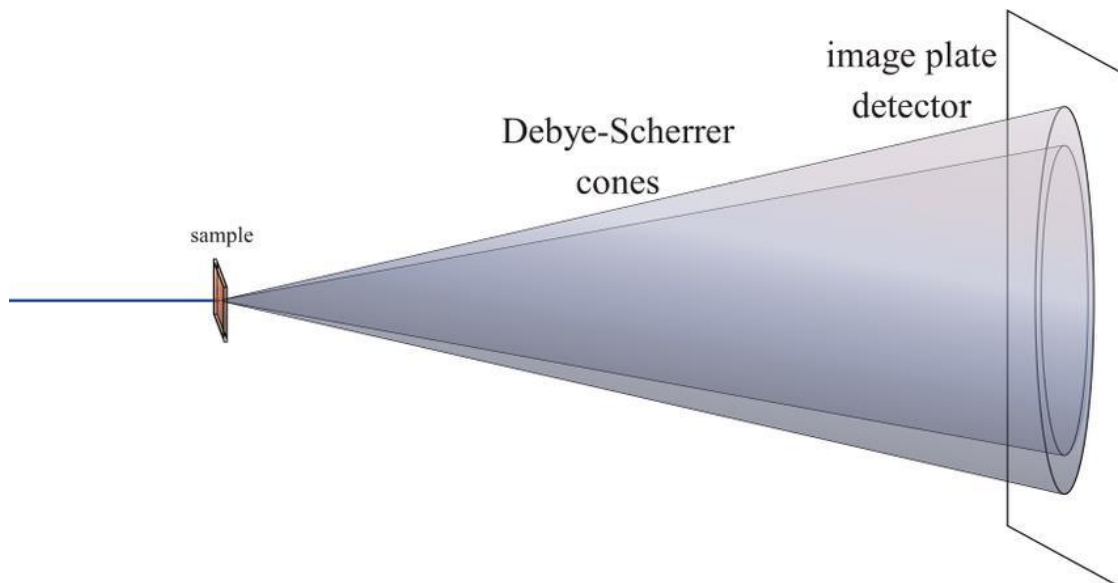


Figure 4.3: Debye scherre cones produced by crystallized material powder and a mono chromatic x-ray beam

4.1.3 Lattice Constant

The lattice constant provides a clear understanding of a crystal unit cell's structural characteristics. A crystalline material's unit cell is characterized by a physical dimension

called the lattice constant, sometimes referred to as the lattice parameter. The complete lattice structure is formed by the length of the edges of the unit cell, the smallest repeating unit in the crystal lattice, when repeated in three dimensions. Specific materials have their own lattice constants, which are useful for distinguishing between various crystalline phases. The following formula can be utilized for calculating lattice constants.

$$d_{hkl} = \frac{a}{\sqrt{h^2 + k^2 + l^2}}$$

4.1.4 Crystallite size

The dimensions of domains within a polycrystalline material that exhibit coherent diffracting are referred to as crystallite size. Since it impacts the chemical and physical properties of materials, it is an essential parameter in the field of materials science. Using the Scherrer equation, X-ray diffraction (XRD) is often utilized to estimate the size of crystallites.

$$D = \frac{K\lambda}{\beta \cos\theta}$$

4.2 Scanning Electron Microscopy:

In these techniques a variety of signals are generated using high energy electron beams. The information derived by electron sample interaction includes surface morphology, orientation, chemical composition, and crystalline structure of the material. Usually a 2-dimensional image is generated showing the surface properties of the samples. Area up to 5 microns can be imaged using scanning electron microscope having resolution from 50 to 100nm in magnification range of 20X to 30000X. Selective analysis can be done through scanning electron microscopy through which we can determine chemical composition using Energy dispersive X- Ray (EDX).

A variety of signals are generated by accelerated electrons interacting with the sample. These signals include secondary electrons (used for determining morphology and topography), backscattered electrons (used for showing contrast in the composition), photons (used for elemental analysis), visible light and heat. SEM is a “non-destructive” technique as production of different signals does not cause volume loss hence same sample can be tested again and again.

To Characterize the nanoparticles, the samples were prepared by sonicating these

nanoparticles in deionized water for 1 to 2 hours. After that a drop of the mixture was poured on a glass slide and then dried at 60° C for 1 hour. Then the glass slide was placed on a stub to gold plate to make the sample conductive and after that the sample was placed in low vacuum chamber to characterize the sample using SEM technique. The image was taken at different magnification and resolution using accelerating voltage of 20 kV.

4.2.1 Fundamental SEM Principle

In scanning electron microscopy, the sample surface is focused under the electron beam. The method utilized is a raster scan, which focuses on extremely small cross section areas. When the concentrated electron beam contacts with a material's surface, the material's surface will release either electrons or photons. To collect the released electrons and photons, several detector sets are used. Detector outputs can be used to control the cathode ray tube's brightness. The cathode ray tubes X and Y inputs are adjusted in accordance with the X and Y voltages to restrain the electron beam. Image 1 was so produced on a cathode ray tube display. Secondary electrons, elemental x-rays, and backscattered electrons all form images.

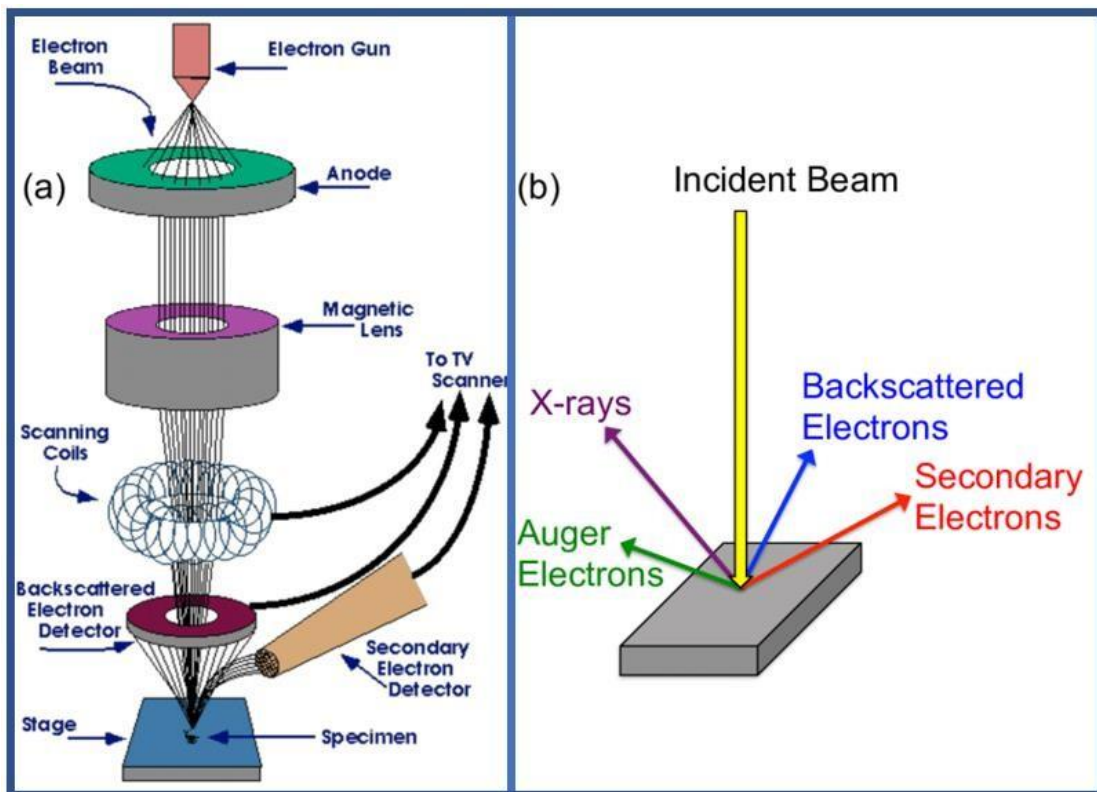


Figure 4.4: (a) Experimental setup of SEM ,(b) Different rays reflected from incident beam

4.3 Fourier-Transform Infrared Spectroscopy (FTIR)

FTIR works on the principle of infrared rays absorbed by the material. The material's ability to absorb infrared light energy at different wavelengths is used to determine molecular structure and composition. FTIR technique is used for the determination of different types of functional groups present on the surface of sample, which is performed in the range of 4000cm^{-1} to 400cm^{-1} using infrared rays from spectrometer. Samples are usually prepared by mixing nanoparticles with potassium bromide (KBr) and then pressing it with the help of uniaxial press into a pellet which is further used for characterization.

4.3.1 Working Principle of FTIR

A polychromatic light source fosters an infrared radiation beam that is directed towards splitters in Fourier Transform Infrared (FTIR) spectroscopy. Half of the incident's light is transmitted through a moving mirror while the other half is refracted towards a stationary mirror. The sample media allows the incident light to travel across it. Information on the molecular makeup and structure of the sample can be obtained by the interaction of the sample with light. Between the visible and microwave portions of the electromagnetic spectrum, infrared rays have wavelengths that are longer than visible and shorter than microwaves. There are three categories for the IR region: far, mid, and near. The infrared portion of the spectrum that is closest to visible light is known as the near infrared. The mid-infrared is the region that is between these near and far spectrums, whilst the far-infrared dimensions refer to the portion that is closer to the microwave range. The primary source of infrared radiation is thermal radiation, which is produced by the mobility of atoms and molecules within the material. More atoms move when the temperature rises, producing more infrared radiation.

The FTIR principle asserts that when the applied IR frequency equals the natural frequency of vibration, absorption of IR radiation results in the production of molecular vibrations. Every distinct bond or functional group has a particular absorption frequency need. As a result, the characteristic peak is seen for each functional group or molecular component.

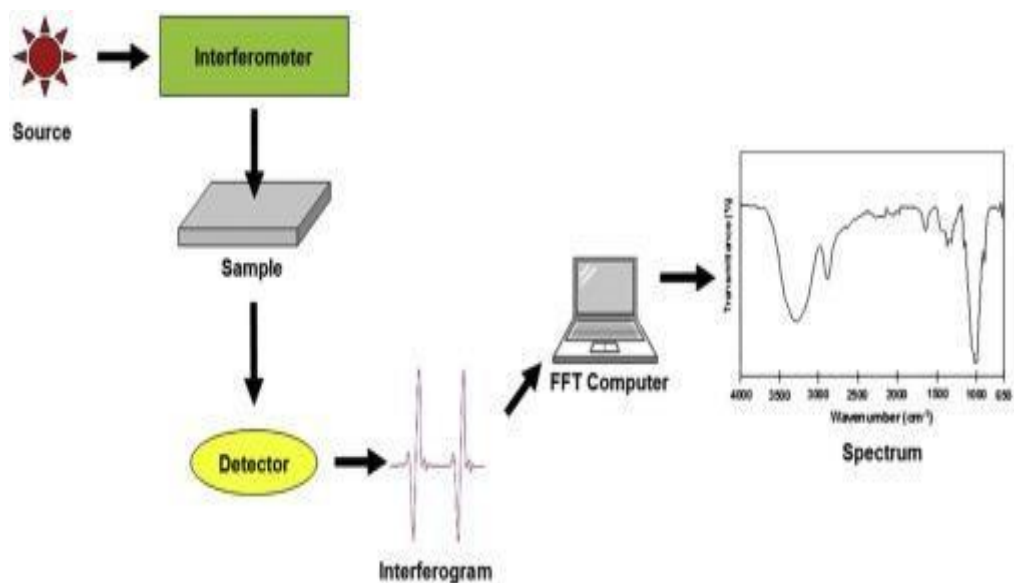


Figure 4.5: FTIR setup

4.4 UV Vis Spectroscopy:

This technique works on the principle of amount of ultraviolet (UV) or visible light absorbed by the sample in comparison to a reference/blank sample providing the information about sample specification (as specific material absorb light at specific wavelength) and its concentration. UV light is usually used for characterizing the sample as UV has wavelengths shorter than visible light hence generating higher energy (frequency). Specific samples have maximum absorbance value at specific wavelength which is used to extract information about the material.

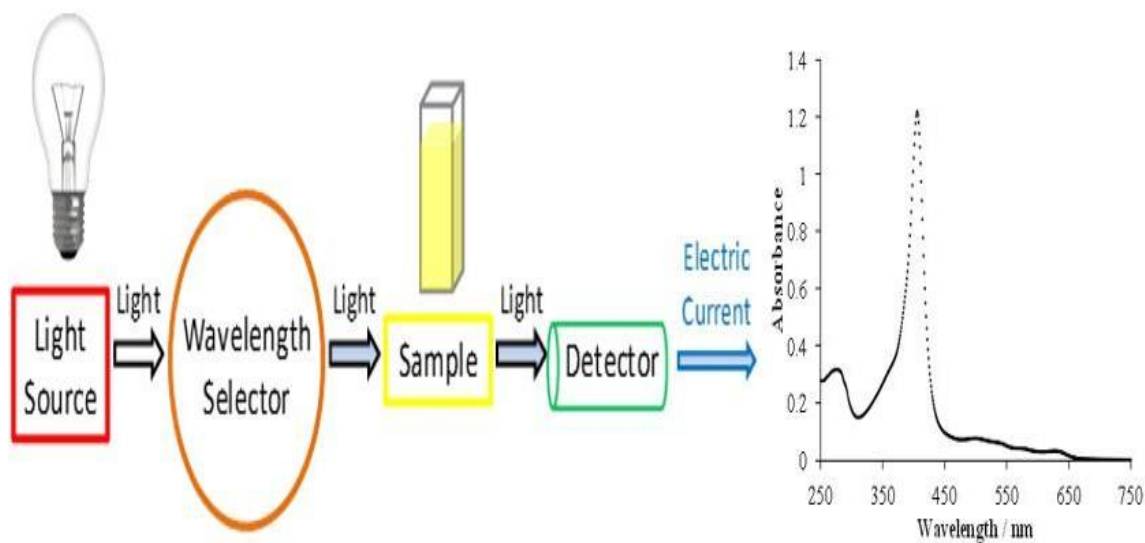


Figure 4.6: Components of UV-Vis spectroscopy

Light source usually of Xenon lamps, a high intensity light source, is used to generate light which is filtered by a monochromator to a desired wavelength and to improve signal to noise ratio which is then passed through a reference sample and from the sample to be tested. Quartz cuvettes are used as sample holders. Initially both reference and main sample cuvettes are filled by the same medium used for filling the sample. After one run, one cuvette containing blank is replaced by a solution containing sample with the same solvent as used before for characterization. The signals generated are detected by a detector and then displayed on a monitor as a graph between absorbance (Y-axis) and wavelength (X-axis).

The absorbance value identified is equal to light intensity (I_0) before passing the sample divided by intensity after passing through the sample (I). The inverse relation of these two quantities gives us the transmission values. The concentration of the sample in mol L⁻¹ could be determined by using Beer-Lambert's law when quantities like molar absorptivity, path length and absorbance values are known.

To characterize the nanoparticles all the samples were dissolved in deionized water with solute to solvent ratio of 1mg/1ml. Quartz cuvettes were used to fill the sample and characterization range of 200-300 nanometer is used.

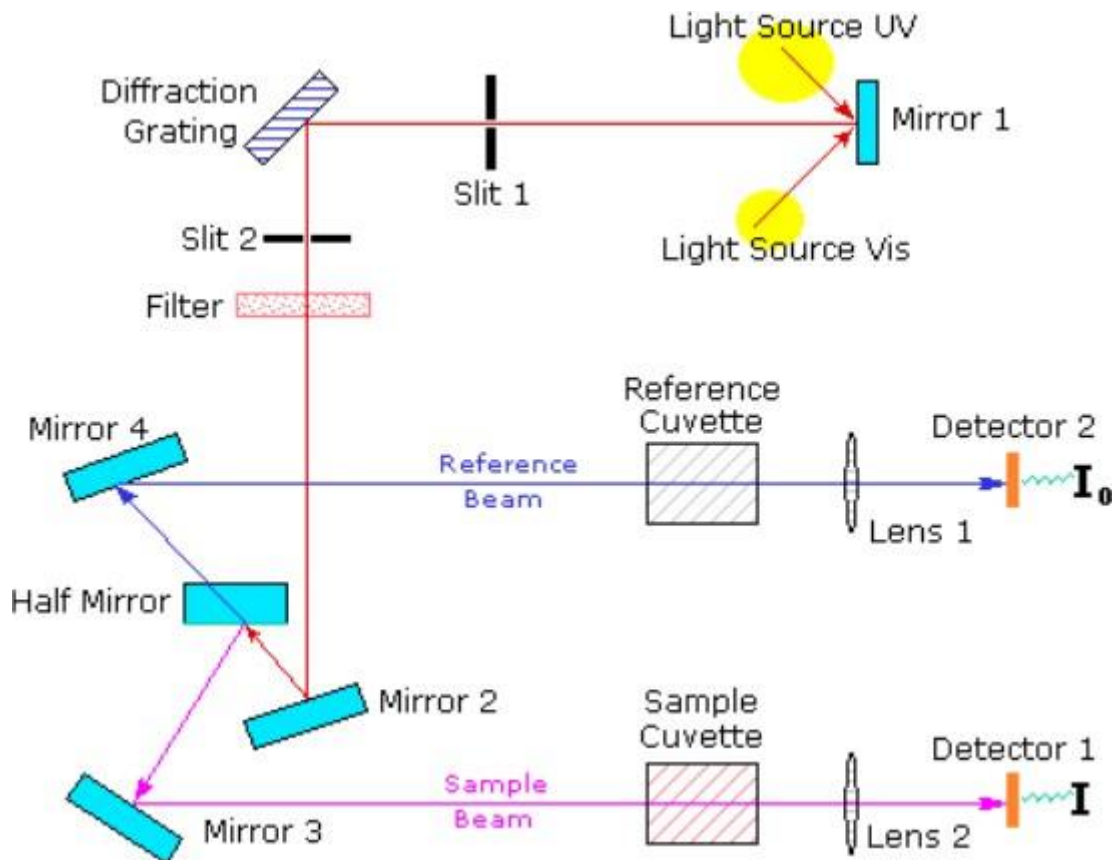


Figure 4.7: Path that UV light takes to pass through reference and sample cuvette

4.5 Hemolysis Testing:

Hemolysis testing involves evaluating how red blood cells (RBCs) respond to various conditions. This includes observing how RBCs swell or shrink in different liquid environments such as hypotonic and hypertonic solutions, assessing their reaction to exposure to different chemicals, testing their resilience to temperature fluctuations, evaluating their ability to withstand mechanical stresses, and determining their resistance to immune system attacks through complement-mediated testing. These tests play a critical role in diagnosing blood disorders, ensuring the safety of blood transfusions, and assessing the impact of medical treatments on blood health.

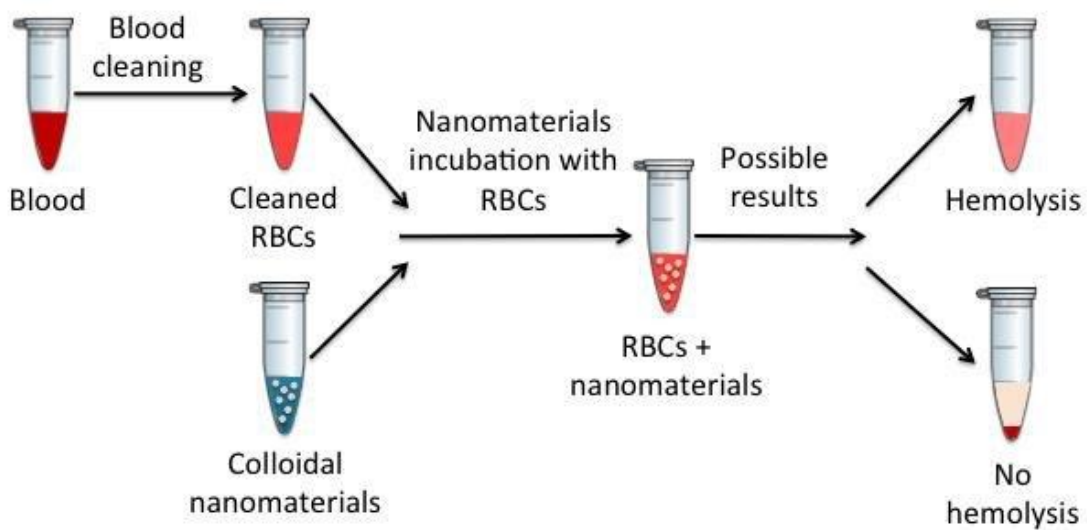


Figure 4.8: Schematic of hemolysis assay

4.5.1 Working Principle of Hemolysis Assay

RBCs preparation

- Blood is utilized, commonly from an animal or human source.
- To separate the RBCs from plasma and other materials, the blood is centrifuged. Any residual plasma is removed from the RBCs by repeatedly washing them in an appropriate buffer solution (phosphate-buffered saline, or PBS).

Working with test sample

- Following washing, the RBCs are further suspended to a predetermined concentration in a buffer solution.
- Multiple concentrations of the test component (e.g., nanoparticles, drug, material) are incorporated with aliquots of the RBC suspension.

- A pair of control samples are made: a positive control (RBCs treated with a known hemolytic agent, such as distilled water or a surfactant) and a negative control (RBCs in buffer alone).

Incubation

- The prepared mixtures are incubated for a specific period (e.g., 1-4 hours) at a physiological temperature, which is normally 37°C.
- Any hemolytic activity of the test substance during this incubation will cause the red blood cells to lyse, releasing hemoglobin into the surrounding solution.

Centrifugation

- To remove any intact RBCs, the samples are centrifuged after incubation.
- The liberated hemoglobin from the lysed cells is collected for evaluation in the supernatant.

Hemoglobin Release Measurement

- Spectrophotometric analysis is used to determine the amount of hemoglobin in the supernatant.
- Certain wavelengths of light—typically those around 540 nm—are absorbed by hemoglobin.
- Each specimen has its absorbance measured, and the amount of hemolysis is determined by contrasting the test samples' absorbance values with those of the controls.

Hemolytic Activity Measurement

- Formula is used to determine the proportion of hemolysis.

$$\text{Hemolysis (\%)} = \frac{\text{Positive control absorbance} - \text{negative control absorbance}}{\text{Test sample absorbance} - \text{negative control absorbance}} \times 100$$

Result interpretation

- A low hemolysis percentage (usually less than 5%) suggests that the test material is safe and has good biocompatibility for use in blood-contacting scenarios.
- A high hemolysis percentage suggests the test material may be unsafe for in vivo use and may be detrimental to RBCs.

CHAPTER 5: RESULTS & DISCUSSION

5.1 XRD Analysis:

The structural modifications of Fe₃O₄ nanoparticles upon the addition of TiO₂ have been explained by X-ray diffraction (XRD) analysis. This includes variations in the overall crystalline structure, the size of the crystallites, lattice constant and the peak intensity, all of which are essential to comprehending the features of the composite in a variety of applications, such as drug delivery.

Figure 5.1 shows the X-ray diffraction patterns of the Fe₃O₄ & Fe₃O₄@TiO₂ synthesized through hydrothermal method. Fe₃O₄ diffraction pattern, displays five distinct Bragg reflections of the magnetite phase at angles 30.44°, 35.79°, 43.42°, 57.46°, and 62.5° corresponds to the planes (220), (311), (400), (422), (511), (440) indicating the formation of inverse cubic spinel structure of Fe₃O₄ [109].

The remaining peaks show reflection at 2θ = 25°, 37°, 47.5°, 54.6°, 62.5°, which corresponds to planes the (101), (004), (200), (211), (204) and reflects a mixture of Fe₃O₄ and TiO₂ anatase phase that forms Fe₃O₄@TiO₂ core shell nanoparticles [110]. Sharper peaks signify an enhanced crystalline structure Fe₃O₄@TiO₂

A drop in the Fe₃O₄ peak's strength has been noticed, which could be related to the TiO₂ layer's impact. A decrease in crystallite size correlated with an increase in the weight percentage of TiO₂. This can be explained by the fact that TiO₂ partially inhibits the agglomeration of Fe₃O₄, resulting in a decrease in crystallite size [111].

In this study crystallite size and lattice constant was calculated using Debye -Scherer formula and Bragg's formula.

$$D = \frac{k\lambda}{\beta \cos\theta}$$

Where, D is crystallite size, K is Scherer's constant, λ is X-ray Wavelength and β is the full width half maximum of the peak and θ is the Bragg angle.

Conversely, the Bragg equation was utilized to determine the d spacing between the XRD peaks, as demonstrated by

$$d = \frac{\lambda}{2\sin\theta}$$

Where, d is d spacing, λ is X-ray Wavelength and θ is the Bragg angle.

The crystallite size and lattice constant of Fe₃O₄ was found to be 13 nm and 8.43 Å respectively.

Table 4. Crystallite size and lattice constant of Fe₃O₄ and Fe₃O₄@TiO₂

| Sample | Crystallite Size (nm) | Lattice Constant Å | |
|---|-----------------------|--------------------|------|
| | | a=b | c |
| Fe ₃ O ₄ @TiO ₂ (5 %) | 13 nm | 3.65 | 9.11 |
| Fe ₃ O ₄ @TiO ₂ (10 %) | 12 nm | 3.69 | 9.21 |
| Fe ₃ O ₄ @TiO ₂ (15 %) | 10nm | 3.79 | 9.24 |
| Fe ₃ O ₄ @TiO ₂ (20 %) | 9.5nm | 3.8 | 9.45 |

The addition of TiO₂ to Fe₃O₄ stabilizes the particles and prevents their excessive shrinking. These findings have effects on applications involving drug delivery. TiO₂ does not change the characteristics of Fe₃O₄, which is important to retain the drug integrity, according to the consistent lattice constant between Fe₃O₄ and Fe₃O₄@TiO₂ nanoparticles. TiO₂ inclusion boosts the nanoparticles' surface area and porosity, offering additional active sites for drug encapsulation. To achieve high drug loading efficiency, high surface area plays vital role. In biological applications, the stability of the nanoparticles can be assured by their high degree of crystallinity. Because stable nanoparticles are less prone to agglomerate, drug delivery systems can operate consistently with them.

Fe₃O₄ nanoparticles with a high degree of crystallinity and an inverse cubic spinel structure were successfully synthesized, as confirmed by the XRD analysis. It is appropriate for drug delivery applications since the predicted lattice constant and crystallite size are consistent with those of conventional magnetite nanoparticles [112]. Additional peaks in the XRD pattern would indicate the existence of TiO₂ in the Fe₃O₄@TiO₂ nanoparticle composite structure, indicating successful composite manufacturing.

Fe₃O₄ and Fe₃O₄@TiO₂ nanoparticles are especially well suited for drug delivery applications due to their structural features, which provide robust, large surface area platforms for effective drug loading and controlled release.

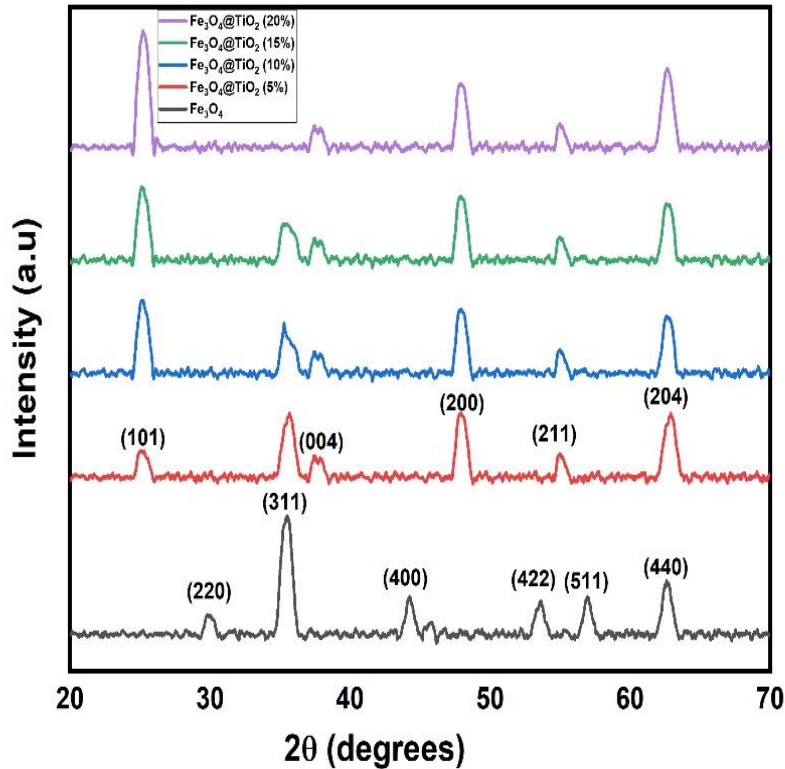


Figure 5.1: XRD pattern of Fe₃O₄ and Fe₃O₄ @ TiO₂ with wt.% (5, 10, 15, 20)

5.2 Scanning Electron Microscopy

5.2.1 Fe₃O₄

The Fe₃O₄ (magnetite) nanoparticles prepared using the hydrothermal method have been evaluated using scanning electron microscopy (SEM) to examine their size distribution and shape. A small quantity of Fe₃O₄ nanoparticles that were synthesized was dissolved in deionized water. After then, the solution was sonicated for an hour. Sonication enables uniform dispersion of the nanoparticles in the solution, avoiding clumping and ensuring a well-distributed sample for SEM. The sample that was successfully sonicated was put on a glass substrate. This substrate offers an adequate foundation for microscopic observations of the nanoparticles.

Gold was coated in a thin layer to the sample. This is an important step because it provides conductive nanoparticles that are needed for SEM testing. Samples that are non-conductive may generate charge when exposed to an electron beam, resulting in distorted images and measurements.

Most of the Fe_3O_4 nanoparticles have a spherical form, as seen by the SEM image. Since spherical particles behave systematically and uniformly, they are useful in a wide range of applications. The pictures demonstrate how small nanoparticles may interact to form larger aggregates. Dipole-dipole interactions, in which the magnetic properties of the nanoparticles cause them to attract each other, are the root cause of this phenomena. The high surface energy and large specific surface area that are inherent to nanoparticles also contribute to agglomeration. One of the typical characteristics of nanoparticles is their tendency to clump together, which could influence how effectively nanoparticles work in certain applications [113].

Image 5.2 exhibit clustering, which is anticipated for bare magnetic nanoparticles. Because of their surface energy and magnetic attraction, magnetic nanoparticles tend to cluster together in the absence of a moderating coating [114]. Most of the nanoparticles are smaller than 100 nm. Considering they may interact with biological systems more effectively and be used for targeted drug delivery, imaging, and other medical applications, particles in the nanometer range are very important for biomedical applications.

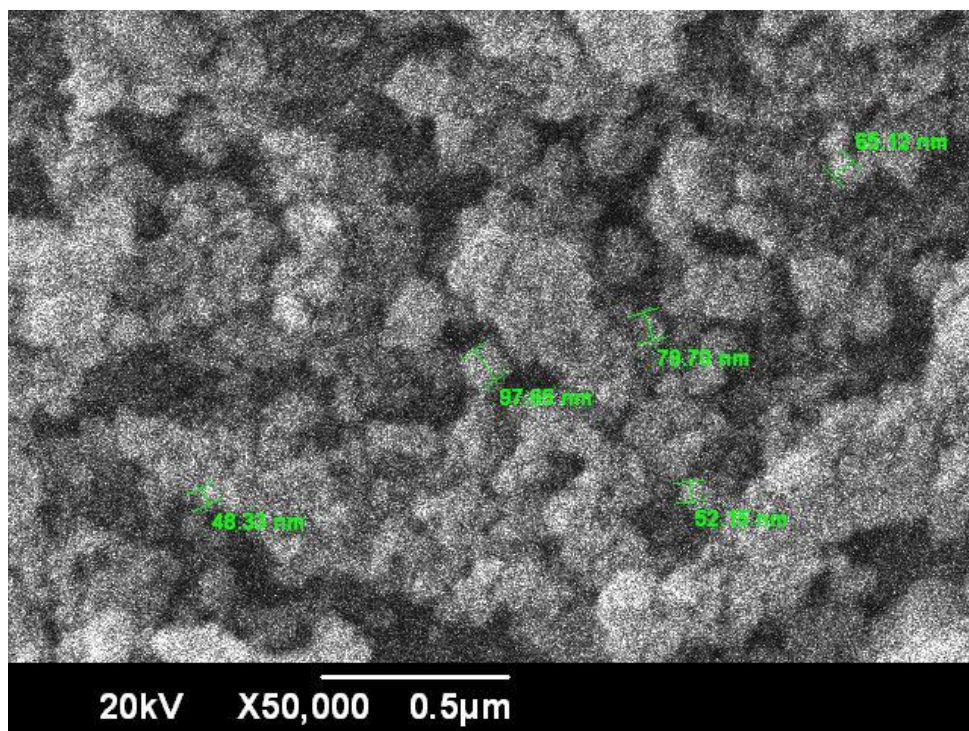


Figure 5.2: SEM of Fe_3O_4

5.2.2 SEM of $\text{Fe}_3\text{O}_4@\text{TiO}_2$

Mechanical mixing was utilized to produce the $\text{Fe}_3\text{O}_4@\text{TiO}_2$ composite nanoparticles, with different TiO_2 ratios (5 %, 10 %, 15 %, and 20 %). Figure 5.3 reveal that the TiO_2

nanoparticles have been effectively incorporated into the Fe_3O_4 matrix. This integration hints to a successful composite production in which TiO_2 content is uniformly distributed in Fe_3O_4 nanoparticles.

The $\text{Fe}_3\text{O}_4@ \text{TiO}_2$ core shell nanoparticles surface looks to be rather smooth with a small amount of roughness. Smoother surfaces may boost interactions with biological systems in biomedical applications, hence this morphological trait is favorable for a variety of biomedical applications.

The aggregation of Fe_3O_4 particles is substantially reduced by the presence of TiO_2 in the composite. TiO_2 acts as a barrier between Fe_3O_4 particles, preventing the particles from clumping together, which as a result responsible for the decrease in agglomeration [115].

The $\text{Fe}_3\text{O}_4@ \text{TiO}_2$ composite nanoparticles are primarily smaller than 100 nm. For biomedical applications, this small size range is highly significant since it enables better cellular penetration and interaction.

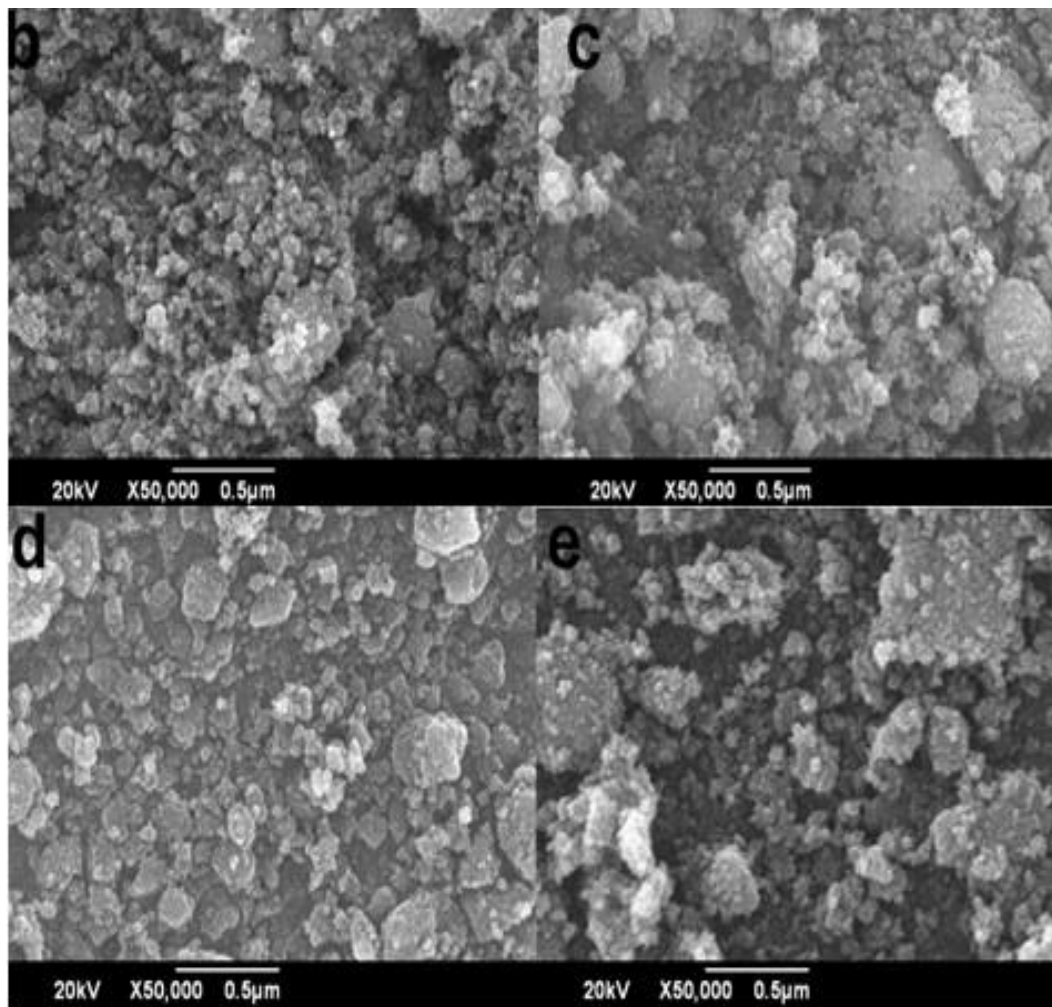


Figure 5.3: SEM of $\text{Fe}_3\text{O}_4 @ \text{TiO}_2$ (b) 5% (c) 10% (d) 15% (e) 20%

5.3 FTIR:

The existence of functional groups that are essential for drug delivery applications, as well as the interactions between the titanium dioxide (TiO_2) shell and the iron oxide (Fe_3O_4) core, are revealed by FTIR analysis, which have been obtained in the $4000\text{--}400\text{ cm}^{-1}$ range.

A peak at 577 cm^{-1} can be seen in the Fe_3O_4 spectra. This peak is caused by the Fe-O stretching vibrations, which are a sign of the magnetite (Fe_3O_4) structure. This indicates that the sample contains magnetite. The presence of adsorbed water molecules on the Fe_3O_4 surface is indicated by the peak 1622 cm^{-1} , which is caused by the hydroxyl groups' bending vibrations.

The broad band spectrum at 3400 cm^{-1} is related to the symmetric and asymmetric stretching vibrations of the O-H bond [116]. It implies that the surface of the nanoparticle comprises of adsorbed water and hydroxyl groups.

The surface hydroxyl groups are likewise responsible for the broad band observed at 3400 cm^{-1} in the $\text{Fe}_3\text{O}_4@\text{TiO}_2$ spectra, just like in the case of Fe_3O_4 . This suggests that the $\text{Fe}_3\text{O}_4@\text{TiO}_2$ nanoparticles' surface contains hydroxyl groups.

Peaks from $1625\text{--}1640\text{ cm}^{-1}$ correspond to molecular water's hydroxyl groups that have been absorbed onto the $\text{Fe}_3\text{O}_4@\text{TiO}_2$ nanoparticles' surface. Interactions between the hydroxyl groups and the TiO_2 covering are suggested by the small shift from 1622 cm^{-1} in Fe_3O_4 to $1625\text{--}1640\text{ cm}^{-1}$ in $\text{Fe}_3\text{O}_4@\text{TiO}_2$.

The band at $500\text{--}900\text{ cm}^{-1}$ indicates the existence of TiO_2 and is caused by the stretching vibrations of Ti-O-Ti. The significantly wider band shows that the $\text{Fe}_3\text{O}_4@\text{TiO}_2$ composite structure has been formed and shows that TiO_2 has successfully attached to the Fe_3O_4 surface. [117]. This band is comparatively wider demonstrating the attachment of TiO_2 to the Fe_3O_4 surface and the successful synthesis of $\text{Fe}_3\text{O}_4@\text{TiO}_2$ [118].

The study's impacts encompass drug delivery applications. The broad band around 3400 cm^{-1} in $\text{Fe}_3\text{O}_4@\text{TiO}_2$ denotes the existence of surface hydroxyl groups, which are essential for improving the nanoparticles' hydrophilicity and biocompatibility. The interaction of water molecules with the surface, indicated by the existence of peaks $1625\text{--}1640\text{ cm}^{-1}$, which affects the drug loading and release behavior. $500\text{--}900\text{ cm}^{-1}$ band's relative width shows that TiO_2 was able to adhere to the Fe_3O_4 surface. The $\text{Fe}_3\text{O}_4@\text{TiO}_2$ composite's production is verified by the presence of this band, which is necessary to improve the nanoparticles' surface characteristics and drug loading ability.

By virtue of the surface hydroxyl groups, $\text{Fe}_3\text{O}_4@\text{TiO}_2$ nanoparticles are more hydrophilic, which improves their dispersion in biological fluids and lowers the risk of aggregation. This characteristic is essential for ensuring the stability and biocompatibility of the nanoparticles in biological contexts.

The drug release kinetics are mostly regulated by the presence of adsorbed water molecules and surface hydroxyl groups, as shown by the FTIR spectrum. These functional groups could hydrogen bond with the drug molecules, resulting in a regulated and sustained release profile that is advantageous for sustaining therapeutic drug levels for a longer amount of time.

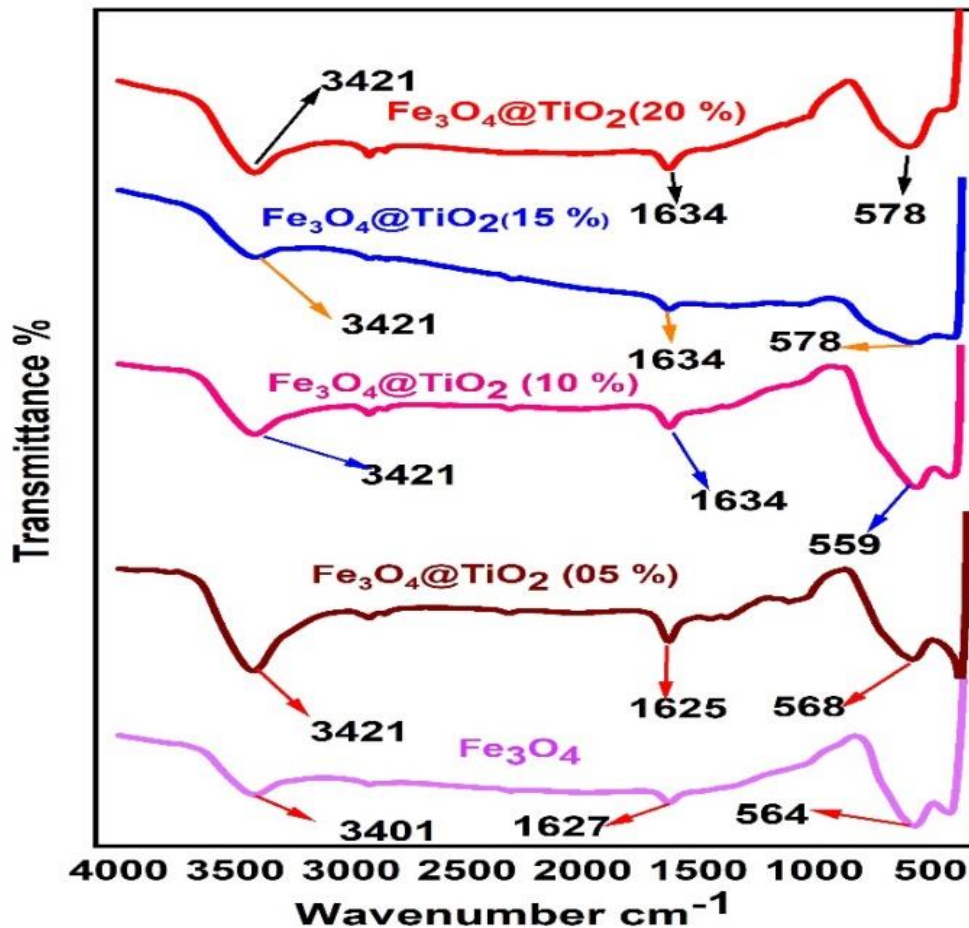


Figure 5.4: FTIR analysis (a) Fe_3O_4 (b) $\text{Fe}_3\text{O}_4 @ \text{TiO}_2$ (5%) (c) $\text{Fe}_3\text{O}_4 @ \text{TiO}_2$ (10%) (d) $\text{Fe}_3\text{O}_4 @ \text{TiO}_2$ (15%) (e) $\text{Fe}_3\text{O}_4 @ \text{TiO}_2$ (20%)

5.4 Drug Loading of Nanoparticles

To assess the synthetic material's efficacy for drug delivery applications, drug loading and release studies were carried out using ciprofloxacin as the drug of choice. The Fe_3O_4 and $\text{Fe}_3\text{O}_4/\text{TiO}_2$ core shell nanoparticles were loaded with ciprofloxacin.

15 mg drug was dispersed in 10 ml of ethanol to yield a 1.5 mg/ml solution, which was then utilized to make the sample. The mixture was centrifuged after stirring for 48 hours. The amount of drug left in the supernatant was measured using a UV-VIS spectrophotometer set to 264 nm wavelength.

5.4.1 Standard Curve of ciprofloxacin:

Four drug dilutions in ethanol have been prepared with concentrations ranging from 0.2 to 0.9 mg/ml for the ciprofloxacin standard curve. A reference curve was obtained at 264 nm to calculate the drug's absorbance for different concentrations.

Table 5. Absorbance values of ciprofloxacin with different concentrations.

| Concentration (mg/ml) | Absorbance |
|--------------------------|------------|
| 0.2 | 0.4859 |
| 0.3 | 0.6513 |
| 0.5 | 0.9798 |
| 0.9 | 1.64589 |

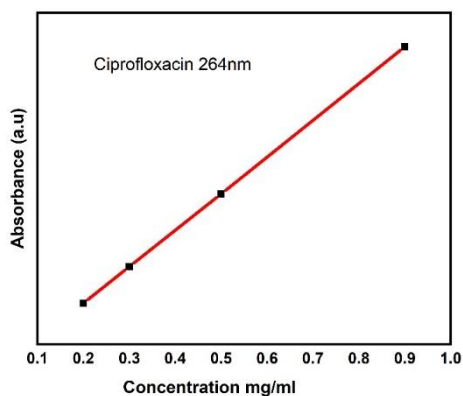


Figure 5.5: Linear curve of ciprofloxacin

5.5 Drug loading on Nanoparticles:

The amount of drug retained in the supernatant was determined using the absorbance value at 264 nm, which was compared to the ciprofloxacin standard curve to calculate the drug's relative amount to that absorbance value.

Encapsulation efficiency of particles was calculated using the following formula:

$$\text{Encapsulation efficiency \%} = \frac{\text{Initial drug weight} - \text{Free drug weight in supernatant}}{\text{Initial drug weight}}$$

Table 6. Encapsulation efficiency (%) of Fe₃O₄ and Fe₃O₄@TiO₂ loaded with Ciprofloxacin

| Sample | Absorbance Value | Initial drug weight (mg/ml) | Relative drug weight (mg/ml) | Encapsulation Efficiency |
|--|------------------|-----------------------------|------------------------------|--------------------------|
| O ₄ | 1.738 | 1.5 | 0.9561 | 36.2 |
| O ₄ @TiO ₂ (5%) | 1.639 | 1.5 | 0.8963 | 40.2 |
| O ₄ @TiO ₂ (10%) | 1.523 | 1.5 | 0.8263 | 44.9 |
| O ₄ @TiO ₂ (15%) | 1.310 | 1.5 | 0.6978 | 53.48 |
| O ₄ @TiO ₂ (20%) | 1.209 | 1.5 | 0.6369 | 57.54 |

Figure 5.6 below displays the encapsulation efficiency of Fe₃O₄ with different weight percent of TiO₂. The encapsulation efficiency of Fe₃O₄ is calculated to be 36.2% and that Fe₃O₄ with TiO₂ (20%) content is 57.54%. It can be seen from the image that increasing TiO₂ wt. % in Fe₃O₄ (magnetite) increases the encapsulation efficiency which can be attributed as TiO₂ has high surface area and porosity which provide more active sites to drug to encapsulate [111, 119]. A larger amount of the drug can be ingested and encapsulated within the nanoparticles because of their larger surface area.

Also, formation of strong bonds (Fe-O-Ti) shows an increase in encapsulation efficiency. Strong Fe-O-Ti connections that form between Fe₃O₄ and TiO₂ improve the nanoparticles' structural stability and integrity. These connections probably let the drug stay in the nanoparticle matrix longer, improving the efficiency of encapsulation.

Improved control over drug release results from higher encapsulation efficiency, which translates into a greater percentage of the delivered drug dose being efficiently packed. Increased encapsulation efficiency can lower the frequency of drug delivery while increasing therapeutic efficacy.

The encapsulation process is significantly influenced by the surface chemistry of TiO_2 , particularly by its interaction with Fe_3O_4 . In addition to increasing encapsulation efficiency, the Fe-O-Ti interactions may stabilize the medication inside the nanoparticle, resulting in extended-release profiles.

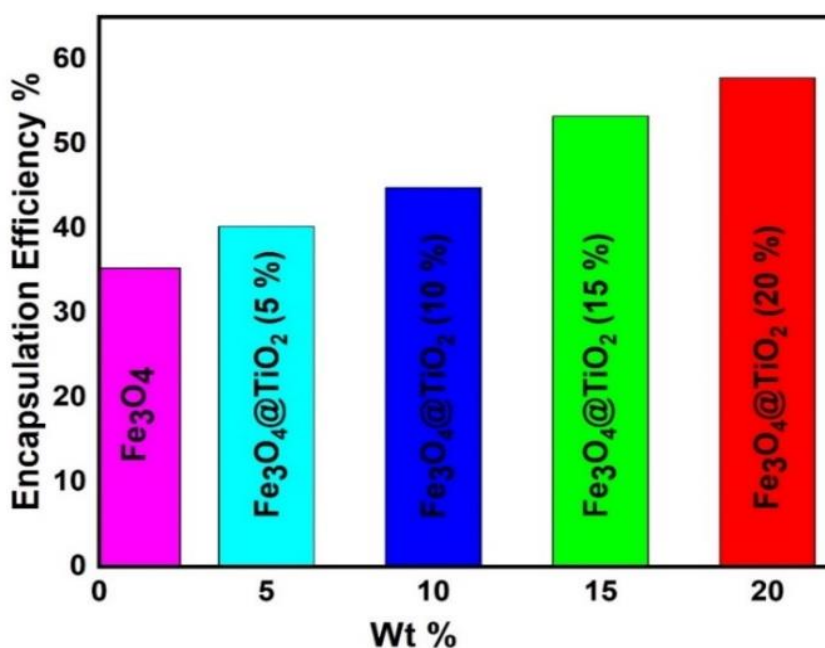


Figure 5.6: Encapsulation efficiency of Fe_3O_4 and $\text{Fe}_3\text{O}_4 @ \text{TiO}_2$ (5%, 10%, 15%, 20%)

5.6 Drug Release Studies of Nanoparticles

To assess the potential of drug-loaded samples, specifically Fe_3O_4 and $\text{Fe}_3\text{O}_4 @ \text{TiO}_2$ nanoparticles, for targeted drug delivery systems, the study explored the in vitro drug release characteristics of these samples.

All drug-loaded samples were subjected to a 24-hour in vitro drug release profile study in pH 7.4 phosphate buffer maintained at 37°C . UV vis absorption spectra at 264 nm were used to calculate the cumulative concentration (CC) of drug release.

The results reveal that $\text{Fe}_3\text{O}_4@\text{TiO}_2$ Wt % 20 exhibits a significant drug release, which is consistent with the notion that it exhibits the maximum encapsulation efficiency. It is clear from the figure that all samples experienced burst drug release during the first 4 hours.

All $\text{Fe}_3\text{O}_4@\text{TiO}_2$ samples drug release profiles indicate superior drug release compared to Fe_3O_4 which showed 55.5 % drug release in 24hrs. It can be seen from the results that 90 % of the drug was released within a time span of 24hrs. This sustained drug release can lead to better targeted drug delivery.

The enhanced percentage of drug release observed in $\text{Fe}_3\text{O}_4@\text{TiO}_2$ during a 24-hour period implies a mechanism of sustained release. For a medication to be therapeutically effective for an extended length of time without requiring frequent dosage changes, sustained release is essential.

$\text{Fe}_3\text{O}_4@\text{TiO}_2$ nanoparticles display enhanced and prolonged drug release, indicating their potential for more precisely targeted drug delivery, less side effects, and better therapeutic efficacy.

Multiple reasons exist for the enhancement of $\text{Fe}_3\text{O}_4@\text{TiO}_2$ nanoparticles in drug release experiments i.e. larger surface area of $\text{Fe}_3\text{O}_4@\text{TiO}_2$ which provide more active sites for drug loading which as a result enhance drug release, improved cumulative release can also be ascribed to improved encapsulation efficiency, which suggests that a larger concentration of the drug is adequately loaded into the nanoparticles and also the uniqueness of material such TiO_2 which shows biocompatibility and stability which may help in higher drug release.

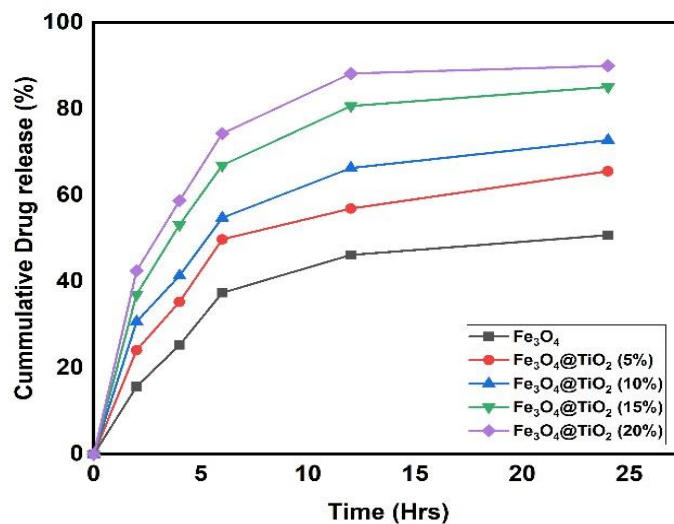


Figure 5.7: Cumulative drug release of Fe_3O_4 and $\text{Fe}_3\text{O}_4 @ \text{TiO}_2$ (5%, 10%, 15%, 20%)

5.7 Hemolysis Assay

The hemolysis assay was conducted to evaluate the biocompatibility of the synthesized Fe_3O_4 and $\text{Fe}_3\text{O}_4@\text{TiO}_2$ nanoparticles for potential drug delivery applications. Red blood cell (RBC) lysis, quantified by hemoglobin release, is a sensitive indicator of material-induced membrane damage [120]. As shown in Figure 5.8, all Fe_3O_4 and $\text{Fe}_3\text{O}_4@\text{TiO}_2$ composites exhibited minimal hemolytic activity at all tested Fe_3O_4 content ratios (5%, 10%, 15%, and 20%). This observation suggests good biocompatibility of the synthesized materials, a crucial prerequisite for their application in drug delivery systems.

These results are in line with previous studies on $\text{Fe}_3\text{O}_4/\text{TiO}_2$ composites. Yang et al. [121] reported minimal hemolysis with $\text{Fe}_3\text{O}_4@\text{TiO}_2$ nanoparticles used for doxorubicin delivery. Similarly, Fu et al. [122] observed negligible hemolytic activity with $\text{Fe}_3\text{O}_4@\text{TiO}_2$ nanoparticles used for curcumin delivery. The low cytotoxicity observed in these studies can be attributed to the synergistic effect of Fe_3O_4 and $\text{Fe}_3\text{O}_4@\text{TiO}_2$ nanoparticles themselves exhibit good biocompatibility due to their inherent biodegradability and similarity to the mineral magnetite found in living organisms [123]. On the other hand, the surface coating of TiO_2 with a proper crystal phase (e.g., anatase) can further minimize cytotoxicity [124].

In the context of drug delivery, the low hemolytic activity of the $\text{Fe}_3\text{O}_4@\text{TiO}_2$ composites is particularly encouraging. It suggests their potential for safe systemic administration, a significant advantage compared to some other nanocarriers that can induce hemolysis [125]. This biocompatibility, coupled with the well-established drug loading and targeting capabilities of $\text{Fe}_3\text{O}_4@\text{TiO}_2$ nanoparticles [126, 127], makes them a promising platform for the development of novel drug delivery systems.

While the hemolysis assay provides valuable insights into initial biocompatibility, further *in vitro* and *in vivo* studies are warranted for a comprehensive assessment. These studies could include cell viability assays with different cell lines, evaluation of long-term toxicity, and biodistribution studies to understand the fate of the nanoparticles within the body.

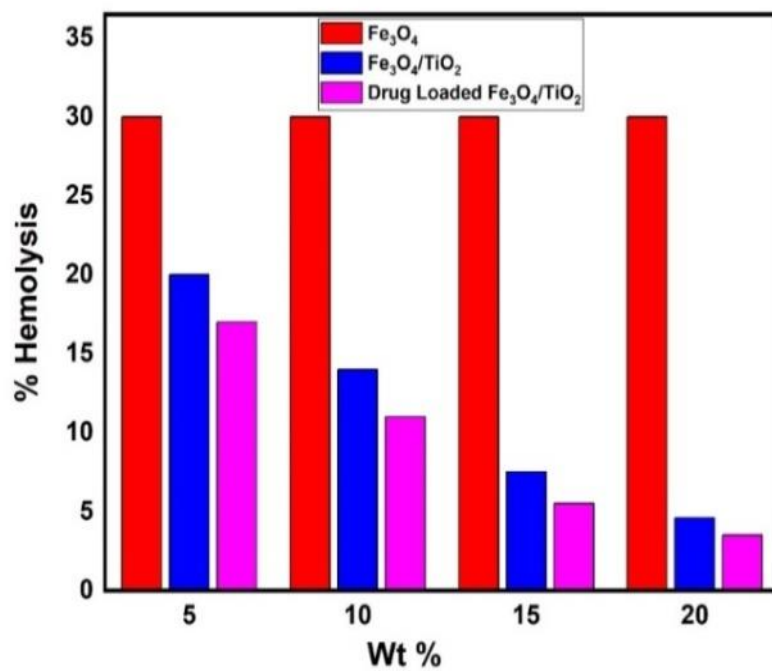


Figure 5.8: Fe₃O₄, Fe₃O₄@ TiO₂ and drug loaded Fe₃O₄ @TiO₂

CHAPTER 6: CONCLUSION

This study involved the synthesis, characterization, and combination of Fe_3O_4 and TiO_2 nanoparticles to create the $\text{Fe}_3\text{O}_4@ \text{TiO}_2$ core-shell structure. The hydrothermal process was utilized for preparing the nanoparticles, and mechanical mixing was used to create the core-shell structure. $\text{Fe}_3\text{O}_4@ \text{TiO}_2$ formation was confirmed by XRD with distinct peaks. The crystallite size ranges between 8-13 nm. SEM morphology was found to be spherical, and the particles size revealed was less than 100 nm making these nanoparticles suitable for biomedical applications especially targeted drug delivery. The functionalized groups of $\text{Fe}_3\text{O}_4@ \text{TiO}_2$ were confirmed by FTIR. Application testing Drug loading & release and hemolysis was observed through UV vis Spectroscopy. The findings of these tests revealed that with 0.2 (20%) ratio of TiO_2 in Fe_3O_4 encapsulation efficiency increased to 55.5 % and the same ratio showed 93% drug release within 24hrs. Hemolytic results show that cytotoxicity is reduced by increasing the TiO_2 ratio which makes it biocompatible and encouraging for drug delivery applications. In general, the $\text{Fe}_3\text{O}_4@ \text{TiO}_2$ nanoparticles showed promising characteristics for applications involving targeted drug administration. It is possible to further optimize their performance by modifying the Fe_3O_4 to TiO_2 ratio.

Future Recommendation

- $\text{Fe}_3\text{O}_4@ \text{TiO}_2$ core-shell nanoparticles have demonstrated encouraging promise for targeted drug delivery due to their special qualities, which include magnetic responsiveness and biocompatibility.
- Future suggestions for improving their efficiency in targeted drug delivery may center on several important areas, including:
 - surface functionalization,
 - drug loading and release optimization and
 - hemocompatibility

REFERENCES:

1. Samrot, A.V., et al., *A review on synthesis, characterization and potential biological applications of superparamagnetic iron oxide nanoparticles*. Current Research in Green and Sustainable Chemistry, 2021. **4**: p. 100042.
2. Davis, S., *Biomedical applications of nanotechnology—implications for drug targeting and gene therapy*. Trends in biotechnology, 1997. **15**(6): p. 217-224.
3. Kim, D., et al., *Synthesis and characterization of surfactant-coated superparamagnetic monodispersed iron oxide nanoparticles*. Journal of magnetism and Magnetic Materials, 2001. **225**(1-2): p. 30-36.
4. Mattox, D.M., *Ion plating—past, present and future*. Surface and Coatings technology, 2000. **133**: p. 517-521.
5. Davino, D. and V.P. Loschiavo, *Numerical Simulation of Magnetic Materials*, in *Encyclopedia of Smart Materials*, A.-G. Olabi, Editor. 2022, Elsevier: Oxford. p. 50-75.
6. Veiseh, O., J.W. Gunn, and M. Zhang, *Design and fabrication of magnetic nanoparticles for targeted drug delivery and imaging*. Advanced drug delivery reviews, 2010. **62**(3): p. 284-304.
7. Vaseghi, S. and S. Mahboubizadeh, *A review on properties and applications of ferrites*. 2023.
8. Dhiman, P., et al., *Basics of Ferrites: Types and Structures*, in *Ferrites and Multiferroics: Fundamentals to Applications*, G.K. Bhargava, et al., Editors. 2021, Springer Singapore: Singapore. p. 1-25.
9. Stäblein, H., *Chapter 7 Hard ferrites and plastoferrites*, in *Handbook of Ferromagnetic Materials*. 1982, Elsevier. p. 441-602.
10. Qin, H., et al., *Spinel ferrites (MFe₂O₄): Synthesis, improvement and catalytic application in environment and energy field*. Advances in Colloid and Interface Science, 2021. **294**: p. 102486.
11. Liandi, A.R., et al., *Recent trends of spinel ferrites (MFe₂O₄: Mn, Co, Ni, Cu, Zn) applications as an environmentally friendly catalyst in multicomponent reactions: A review*. Case Studies in Chemical and Environmental Engineering, 2023. **7**: p. 100303.
12. Nur, E.A.M., et al., *Properties of Ferrite Garnet (Bi, Lu, Y)₃(Fe, Ga)₅O₁₂ Thin Film Materials Prepared by RF Magnetron Sputtering*. LID - 10.3390/nano8050355 [doi] LID - 355. (2079-4991 (Print)).
13. Kong, L.B., et al., *15 - Theory of ferrimagnetism and ferrimagnetic metal oxides*, in *Magnetic, Ferroelectric, and Multiferroic Metal Oxides*, B.D. Stojanovic, Editor. 2018, Elsevier. p. 287-311.

14. Thorek, D.L., et al., *Superparamagnetic iron oxide nanoparticle probes for molecular imaging*. *Annals of biomedical engineering*, 2006. **34**: p. 23-38.
15. Lee, S.J., et al., *Synthesis of highly magnetic graphite-encapsulated FeCo nanoparticles using a hydrothermal process*. *Nanotechnology*, 2011. **22**(37): p. 375603.
16. Chiang, P.-C., et al., *Engineering water-dispersible FePt nanoparticles for biomedical applications*. *IEEE transactions on magnetics*, 2007. **43**(6): p. 2445-2447.
17. Doaga, A., et al., *Synthesis and characterizations of manganese ferrites for hyperthermia applications*. *Materials Chemistry and Physics*, 2013. **143**(1): p. 305-310.
18. Joshi, H.M., et al., *Effects of shape and size of cobalt ferrite nanostructures on their MRI contrast and thermal activation*. *The Journal of Physical Chemistry C*, 2009. **113**(41): p. 17761-17767.
19. Corbierre, M.K., J. Beerens, and R.B. Lennox, *Gold nanoparticles generated by electron beam lithography of gold (I)- thiolate thin films*. *Chemistry of materials*, 2005. **17**(23): p. 5774-5779.
20. Tseng, A.A., et al., *Electron beam lithography in nanoscale fabrication: recent development*. *IEEE Transactions on electronics packaging manufacturing*, 2003. **26**(2): p. 141-149.
21. Manfrinato, V.R., et al., *Resolution limits of electron-beam lithography toward the atomic scale*. *Nano letters*, 2013. **13**(4): p. 1555-1558.
22. Yang, G., *Laser ablation in liquids: Applications in the synthesis of nanocrystals*. *Progress in Materials Science*, 2007. **52**(4): p. 648-698.
23. Amendola, V. and M. Meneghetti, *Laser ablation synthesis in solution and size manipulation of noble metal nanoparticles*. *Physical chemistry chemical physics*, 2009. **11**(20): p. 3805-3821.
24. Willmott, P. and J. Huber, *Pulsed laser vaporization and deposition*. *Reviews of Modern Physics*, 2000. **72**(1): p. 315.
25. Ling, D. and T. Hyeon, *Chemical design of biocompatible iron oxide nanoparticles for medical applications*. *Small*, 2013. **9**(9- 10): p. 1450-1466.
26. Bomati-Miguel, O., et al., *Calorimetric study of maghemite nanoparticles synthesized by laser-induced pyrolysis*. *Chemistry of Materials*, 2008. **20**(2): p. 591-598.
27. Cao, W., *Synthesis of nanomaterials by high energy ball milling*. Skyspring Nanomaterials, Inc, 2007.
28. Fokina, E., et al., *Planetary mills of periodic and continuous action*. *Journal of Materials Science*, 2004. **39**: p. 5217-5221.

29. Ahn, T., et al., *Formation pathways of magnetite nanoparticles by coprecipitation method*. The journal of physical chemistry C, 2012. **116**(10): p. 6069-6076.
30. Mosafer, J., et al., *Preparation and characterization of uniform-sized PLGA nanospheres encapsulated with oleic acid-coated magnetic-Fe₃O₄ nanoparticles for simultaneous diagnostic and therapeutic applications*. Colloids and Surfaces A: Physicochemical and Engineering Aspects, 2017. **514**: p. 146-154.
31. Hayashi, H. and Y. Hakuta, *Hydrothermal synthesis of metal oxide nanoparticles in supercritical water*. Materials, 2010. **3**(7): p. 3794-3817.
32. Rane, A.V., et al., *Methods for synthesis of nanoparticles and fabrication of nanocomposites*, in *Synthesis of inorganic nanomaterials*. 2018, Elsevier. p. 121-139.
33. Chikan, V. and E.J. McLaurin, *Rapid nanoparticle synthesis by magnetic and microwave heating*. Nanomaterials, 2016. **6**(5): p. 85.
34. Palomino, R., et al., *Sonochemical assisted synthesis of SrFe₁₂O₁₉ nanoparticles*. Ultrasonics sonochemistry, 2016. **29**: p. 470-475.
35. ABHILASH, K. Revati, and B. Pandey, *Microbial synthesis of iron-based nanomaterials—A review*. Bulletin of Materials Science, 2011. **34**: p. 191-198.
36. Iravani, S., *Green synthesis of metal nanoparticles using plants*. Green chemistry, 2011. **13**(10): p. 2638-2650.
37. Arami, H., et al., *In vivo delivery, pharmacokinetics, biodistribution and toxicity of iron oxide nanoparticles*. Chemical Society Reviews, 2015. **44**(23): p. 8576-8607.
38. Senyei, A., K. Widder, and G. Czerlinski, *Magnetic guidance of drug-carrying microspheres*. Journal of Applied Physics, 1978. **49**(6): p. 3578-3583.
39. McNamara, K. and S.A. Tofail, *Nanoparticles in biomedical applications*. Advances in Physics: X, 2017. **2**(1): p. 54-88.
40. Sun, C., J.S. Lee, and M. Zhang, *Magnetic nanoparticles in MR imaging and drug delivery*. Advanced drug delivery reviews, 2008. **60**(11): p. 1252-1265.
41. Mahmoudi, M., et al., *Superparamagnetic iron oxide nanoparticles (SPIONs): development, surface modification and applications in chemotherapy*. Advanced drug delivery reviews, 2011. **63**(1-2): p. 24-46.
42. Maleki, H., et al., *Size-controlled synthesis of superparamagnetic iron oxide nanoparticles and their surface coating by gold for biomedical applications*. Journal of Magnetism and Magnetic Materials, 2012. **324**(23): p. 3997-4005.
43. Faraji, M., Y. Yamini, and M. Rezaee, *Magnetic nanoparticles: synthesis, stabilization, functionalization, characterization, and applications*. Journal of

the Iranian Chemical Society, 2010. **7**: p. 1-37.

44. Teja, A.S. and P.-Y. Koh, *Synthesis, properties, and applications of magnetic iron oxide nanoparticles*. Progress in crystal growth and characterization of materials, 2009. **55**(1-2): p. 22-45.
45. Rafi, M.M., et al., *Synthesis, characterization and magnetic properties of hematite (α -Fe₂O₃) nanoparticles on polysaccharide templates and their antibacterial activity*. Applied Nanoscience, 2015. **5**(4): p. 515-520.
46. Singh, H., et al., *Development of superparamagnetic iron oxide nanoparticles via direct conjugation with ginsenosides and its in-vitro study*. Journal of Photochemistry and Photobiology B: Biology, 2018. **185**: p. 100-110.
47. Zysler, R., D. Fiorani, and A. Testa, *Investigation of magnetic properties of interacting Fe₂O₃ nanoparticles*. Journal of magnetism and magnetic materials, 2001. **224**(1): p. 5-11.
48. Cornell, R.M. and U. Schwertmann, *The iron oxides: structure, properties, reactions, occurrences, and uses*. Vol. 664. 2003: Wiley-vch Weinheim.
49. Champagne, P.-O., et al., *Colloidal stability of superparamagnetic iron oxide nanoparticles in the central nervous system: a review*. Nanomedicine, 2018. **13**(11): p. 1385-1400.
50. Samrot, A.V., et al., *Current Research in Green and Sustainable Chemistry*. 2021.
51. Mahmoudi, M., et al., *Toxicity evaluations of superparamagnetic iron oxide nanoparticles: cell "vision" versus physicochemical properties of nanoparticles*. ACS nano, 2011. **5**(9): p. 7263-7276.
52. Kandasamy, G. and D. Maity, *Recent advances in superparamagnetic iron oxide nanoparticles (SPIONs) for in vitro and in vivo cancer nanotheranostics*. International journal of pharmaceutics, 2015. **496**(2): p. 191-218.
53. Sun, Y.-P., et al., *Characterization of zero-valent iron nanoparticles*. Advances in colloid and interface science, 2006. **120**(1-3): p. 47-56.
54. Bi, L., et al., *Magneto-optical thin films for on-chip monolithic integration of non-reciprocal photonic devices*. Materials, 2013. **6**(11): p. 5094-5117.
55. Bautista, M., et al., *Comparative study of ferrofluids based on dextran-coated iron oxide and metal nanoparticles for contrast agents in magnetic resonance imaging*. Nanotechnology, 2004. **15**(4): p. S154.
56. Gupta, A.K., et al., *Recent advances on surface engineering of magnetic iron oxide nanoparticles and their biomedical applications*. 2007.
57. Nam, J., et al., *Surface engineering of inorganic nanoparticles for imaging and therapy*. Advanced drug delivery reviews, 2013. **65**(5): p. 622-648.

58. Gupta, A.K. and A.S. Curtis, *Surface modified superparamagnetic nanoparticles for drug delivery: interaction studies with human fibroblasts in culture*. Journal of Materials Science: Materials in Medicine, 2004. **15**(4): p. 493-496.
59. Fahmy, H.M., et al., *Review of green methods of iron nanoparticles synthesis and applications*. BioNanoScience, 2018. **8**: p. 491-503.
60. Thorn, C.F., et al., *Doxorubicin pathways: pharmacodynamics and adverse effects*. Pharmacogenetics and genomics, 2011. **21**(7): p. 440-446.
61. Kampan, N.C., et al., *Paclitaxel and its evolving role in the management of ovarian cancer*. BioMed research international, 2015. **2015**.
62. Quan, Q., et al., *HSA coated iron oxide nanoparticles as drug delivery vehicles for cancer therapy*. Molecular pharmaceutics, 2011. **8**(5): p. 1669-1676.
63. Dasari, S. and P.B. Tchounwou, *Cisplatin in cancer therapy: molecular mechanisms of action*. European journal of pharmacology, 2014. **740**: p. 364-378.
64. Chen, D., et al., *Bortezomib as the first proteasome inhibitor anticancer drug: current status and future perspectives*. Current cancer drug targets, 2011. **11**(3): p. 239-253.
65. Xie, J., et al., *Human serum albumin coated iron oxide nanoparticles for efficient cell labeling*. Chemical Communications, 2010. **46**(3): p. 433-435.
66. Huang, Y., et al., *Superparamagnetic iron oxide nanoparticles conjugated with folic acid for dual target-specific drug delivery and MRI in cancer theranostics*. Materials Science and Engineering: C, 2017. **70**: p. 763-771.
67. Yang, Y., et al., *Doxorubicin-conjugated heparin-coated superparamagnetic iron oxide nanoparticles for combined anticancer drug delivery and magnetic resonance imaging*. Journal of biomedical nanotechnology, 2016. **12**(11): p. 1963-1974.
68. Issa, B., et al., *Magnetic nanoparticles: surface effects and properties related to biomedicine applications*. International journal of molecular sciences, 2013. **14**(11): p. 21266-21305.
69. Wagstaff, A.J., et al., *Cisplatin drug delivery using gold-coated iron oxide nanoparticles for enhanced tumour targeting with external magnetic fields*. Inorganica Chimica Acta, 2012. **393**: p. 328-333.
70. Hornung, A., et al., *Treatment efficiency of free and nanoparticle-loaded mitoxantrone for magnetic drug targeting in multicellular tumor spheroids*. Molecules, 2015. **20**(10): p. 18016-18030.
71. Nadeem, M., et al., *Magnetic properties of polyvinyl alcohol and doxorubicine loaded iron oxide nanoparticles for anticancer drug delivery applications*. PloS one, 2016. **11**(6): p. e0158084.

72. Zaloga, J., et al., *Development of a lauric acid/albumin hybrid iron oxide nanoparticle system with improved biocompatibility*. International journal of nanomedicine, 2014: p. 4847-4866.
73. Natesan, S., et al., *Artemisinin loaded chitosan magnetic nanoparticles for the efficient targeting to the breast cancer*. International journal of biological macromolecules, 2017. **104**: p. 1853-1859.
74. Jeon, H., et al., *Poly-paclitaxel/cyclodextrin-SPION nano-assembly for magnetically guided drug delivery system*. Journal of controlled release, 2016. **231**: p. 68-76.
75. Lee, G.Y., et al., *Theranostic nanoparticles with controlled release of gemcitabine for targeted therapy and MRI of pancreatic cancer*. ACS nano, 2013. **7**(3): p. 2078-2089.
76. Mu, Q., et al., *Anti-HER2/neu peptide-conjugated iron oxide nanoparticles for targeted delivery of paclitaxel to breast cancer cells*. Nanoscale, 2015. **7**(43): p. 18010-18014.
77. Ahmed, M.S.U., et al., *Double-receptor-targeting multifunctional iron oxide nanoparticles drug delivery system for the treatment and imaging of prostate cancer*. International journal of nanomedicine, 2017: p. 6973-6984.
78. Nagesh, P.K., et al., *PSMA targeted docetaxel-loaded superparamagnetic iron oxide nanoparticles for prostate cancer*. Colloids and Surfaces B: Biointerfaces, 2016. **144**: p. 8-20.
79. Leach, J.C., et al., *A RNA-DNA hybrid aptamer for nanoparticle-based prostate tumor targeted drug delivery*. International journal of molecular sciences, 2016. **17**(3): p. 380.
80. Arias, L.S., et al., *Iron oxide nanoparticles for biomedical applications: a perspective on synthesis, drugs, antimicrobial activity, and toxicity*. Antibiotics, 2018. **7**(2): p. 46.
81. Mura, S., J. Nicolas, and P. Couvreur, *Stimuli-responsive nanocarriers for drug delivery*. Nature materials, 2013. **12**(11): p. 991-1003.
82. Kievit, F.M., et al., *Doxorubicin loaded iron oxide nanoparticles overcome multidrug resistance in cancer in vitro*. Journal of controlled release, 2011. **152**(1): p. 76-83.
83. Gautier, J., et al., *A pharmaceutical study of doxorubicin-loaded PEGylated nanoparticles for magnetic drug targeting*. International journal of pharmaceutics, 2012. **423**(1): p. 16-25.
84. Wimardhani, Y.S., et al., *Chitosan exerts anticancer activity through induction of apoptosis and cell cycle arrest in oral cancer cells*. Journal of oral science, 2014. **56**(2): p. 119-126.
85. Unsoy, G., et al., *Chitosan magnetic nanoparticles for pH responsive*

- Bortezomib release in cancer therapy*. Biomedicine & Pharmacotherapy, 2014. **68**(5): p. 641-648.
86. Unsoy, G., et al., *Synthesis of Doxorubicin loaded magnetic chitosan nanoparticles for pH responsive targeted drug delivery*. European Journal of Pharmaceutical Sciences, 2014. **62**: p. 243-250.
 87. Adimoolam, M.G., et al., *A simple approach to design chitosan functionalized Fe₃O₄ nanoparticles for pH responsive delivery of doxorubicin for cancer therapy*. Journal of Magnetism and Magnetic Materials, 2018. **448**: p. 199-207.
 88. Zou, Y., et al., *Doxorubicin-loaded mesoporous magnetic nanoparticles to induce apoptosis in breast cancer cells*. Biomedicine & Pharmacotherapy, 2015. **69**: p. 355-360.
 89. Rajh, T., et al., *Titanium dioxide in the service of the biomedical revolution*. Chemical reviews, 2014. **114**(19): p. 10177-10216.
 90. Gohari, G., et al., *Titanium dioxide nanoparticles (TiO₂ NPs) promote growth and ameliorate salinity stress effects on essential oil profile and biochemical attributes of *Dracocephalum moldavica**. Scientific reports, 2020. **10**(1): p. 912.
 91. Logan, N., et al., *TiO₂-coated CoCrMo: Improving the osteogenic differentiation and adhesion of mesenchymal stem cells in vitro*. Journal of Biomedical Materials Research Part A, 2015. **103**(3): p. 1208-1217.
 92. Almeida, M.M., et al., *Strontium ranelate increases osteoblast activity*. Tissue and Cell, 2016. **48**(3): p. 183-188.
 93. Wang, T., et al., *Potential application of functional porous TiO₂ nanoparticles in light-controlled drug release and targeted drug delivery*. Acta biomaterialia, 2015. **13**: p. 354-363.
 94. Wang, Q., et al., *TiO₂ nanotube platforms for smart drug delivery: a review*. International journal of nanomedicine, 2016: p. 4819-4834.
 95. Jafari, S., et al., *Biomedical applications of TiO₂ nanostructures: recent advances*. International journal of nanomedicine, 2020: p. 3447-3470.
 96. Torres, C.C., et al., *PAMAM-grafted TiO₂ nanotubes as novel versatile materials for drug delivery applications*. Materials Science and Engineering: C, 2016. **65**: p. 164-171.
 97. Salahuddin, N., et al., *Synthesis and Design of Norfloxacin drug delivery system based on PLA/TiO₂ nanocomposites: Antibacterial and antitumor activities*. Materials Science and Engineering: C, 2020. **108**: p. 110337.
 98. Shojaie Chahregh, H. and S. Dinarvand, *TiO₂-Ag/blood hybrid nanofluid flow through an artery with applications of drug delivery and blood circulation in the respiratory system*. International Journal of Numerical Methods for Heat & Fluid Flow, 2020. **30**(11): p. 4775-4796.

99. Abbasi, A., *Chapter 7 - TiO₂-Based Nanocarriers for Drug Delivery*, in *Nanocarriers for Drug Delivery*, S.S. Mohapatra, et al., Editors. 2019, Elsevier. p. 205-248.
100. Zhao, J., et al., *NIR Light-Driven Photocatalysis on Amphiphilic TiO₂ Nanotubes for Controllable Drug Release*. ACS Applied Materials & Interfaces, 2020. **12**(20): p. 23606-23616.
101. He, X., et al., *Biocompatibility, corrosion resistance and antibacterial activity of TiO₂/CuO coating on titanium*. Ceramics International, 2017. **43**(18): p. 16185-16195.
102. Ikono, R., et al., *Enhanced bone regeneration capability of chitosan sponge coated with TiO₂ nanoparticles*. Biotechnology Reports, 2019. **24**: p. e00350.
103. Jiang, Z., et al., *An effective light activated TiO₂ nanodot platform for gene delivery within cell sheets to enhance osseointegration*. Chemical Engineering Journal, 2020. **402**: p. 126170.
104. Liu, Y., et al., *A novel microwave stimulus remote-controlled anticancer drug release system based on Janus TiO₂-x&mSiO₂ nanocarriers*. Materials Science and Engineering: C, 2021. **123**: p. 111968.
105. Yilmaz, E. and M. Soylak, *15 - Functionalized nanomaterials for sample preparation methods*, in *Handbook of Nanomaterials in Analytical Chemistry*, C. Mustansar Hussain, Editor. 2020, Elsevier. p. 375-413.
106. Srivastava, A. and A. Katiyar, *10 - Zinc oxide nanostructures*, in *Ceramic Science and Engineering*, K.P. Misra and R.D.K. Misra, Editors. 2022, Elsevier. p. 235-262.
107. Kafle, B.P., *Chapter 6 - Introduction to nanomaterials and application of UV-Visible spectroscopy for their characterization*, in *Chemical Analysis and Material Characterization by Spectrophotometry*, B.P. Kafle, Editor. 2020, Elsevier. p. 147-198.
108. Denkbař, E.B., et al., *Chapter 9 - Magnetically based nanocarriers in drug delivery*, in *Nanobiomaterials in Drug Delivery*, A.M. Grumezescu, Editor. 2016, William Andrew Publishing. p. 285-331.
109. Beyene, M., et al., *A C-Doped TiO₂/Fe₃O₄ Nanocomposite for Photocatalytic Dye Degradation under Natural Sunlight Irradiation*. 2019. **3**: p. 11.
110. Azizi-Lalabadi, M., et al., *Antimicrobial activity of Titanium dioxide and Zinc oxide nanoparticles supported in 4A zeolite and evaluation the morphological characteristic*. Scientific Reports, 2019. **9**(1): p. 17439.
111. Cui, X.-g., et al., *Porous Titanium Dioxide Spheres for Drug Delivery and Sustained Release*. Frontiers in Materials, 2021. **8**.
112. Mushtaq, F., et al., *Preparation, properties, and applications of gelatin-based hydrogels (GHs) in the environmental, technological, and biomedical sectors*.

- International Journal of Biological Macromolecules, 2022. **218**: p. 601-633.
113. Simamora, P., et al., *The Structural and Morphology Properties of Fe₃O₄/Ppy Nanocomposite*. Journal of Physics: Conference Series, 2018. **1120**(1): p. 012063.
 114. Ni, S., et al., *Hydrothermal synthesis of Fe₃O₄ nanoparticles and its application in lithium ion battery*. Materials Letters, 2009. **63**(30): p. 2701-2703.
 115. Chen, X.-Q., H.-X. Zhang, and W.-H. Shen, *Preparation and characterization of the magnetic Fe₃O₄@TiO₂ nanocomposite with the in-situ synthesis coating method*. Materials Chemistry and Physics, 2018. **216**: p. 496-501.
 116. Husain, S., et al., *Synthesis and characterization of Fe₃O₄ magnetic nanoparticles from iron ore*. Journal of Physics: Conference Series, 2019. **1242**(1): p. 012021.
 117. Ma, P., et al., *Synthesis and photocatalytic property of Fe₃O₄@TiO₂ core/shell nanoparticles supported by reduced graphene oxide sheets*. Journal of Alloys and Compounds, 2013. **578**: p. 501-506.
 118. Khashan, S., et al., *Novel method for synthesis of Fe₃O₄@TiO₂ core/shell nanoparticles*. Surface and Coatings Technology, 2017. **322**: p. 92-98.
 119. Lin, H.K., et al., *Chapter 3 - Synthesis of nanomaterials using bottom-up methods*, in *Advanced Nanomaterials and Their Applications in Renewable Energy (Second Edition)*, J.L. Liu, T.-H. Yan, and S. Bashir, Editors. 2022, Elsevier. p. 61-110.
 120. Cohen, E.N., et al., *Carbon dots as nanotherapeutics for biomedical application*. 2020. **26**(19): p. 2207-2221.
 121. Shen, S., et al., *Core-shell structured Fe₃O₄@ TiO₂-doxorubicin nanoparticles for targeted chemo-sonodynamic therapy of cancer*. 2015. **486**(1-2): p. 380-388.
 122. Wang, B., et al., *Novel Fe₃O₄@ TiO₂ core-shell nanostructure catalyst for NO removal through heterogeneous Fenton processes*. 2024. **434**: p. 140100.
 123. Xu, Y., et al., *Multifunctional Fe₃O₄@ C-based nanoparticles coupling optical/MRI imaging and pH/photothermal controllable drug release as efficient anti-cancer drug delivery platforms*. 2019. **30**(42): p. 425102.
 124. Jamil, S. and M.J.M.I. Fasehullah, *Effect of temperature on structure, morphology, and optical properties of TiO₂ nanoparticles*. 2021. **1**(01): p. 22-8.
 125. Tremblay-McLean, A., et al., *Expression profiles of ligands for activating natural killer cell receptors on HIV infected and uninfected CD4⁺ T cells*. 2017. **9**(10): p. 295.

126. Ma, W.-F., et al., *Tailor-made magnetic Fe₃O₄@ mTiO₂ microspheres with a tunable mesoporous anatase shell for highly selective and effective enrichment of phosphopeptides*. 2012. **6**(4): p. 3179-3188.
127. Abbas, M., et al., *Fe₃O₄/TiO₂ core/shell nanocubes: Single-batch surfactantless synthesis, characterization and efficient catalysts for methylene blue degradation*. 2014. **40**(7): p. 11177-11186.